Stony Brook University

Title of Thesis

A Thesis Presented

by

Wenbo Wang

to

The Graduate School

in Partial Fulfillment of the

Requirements

for the Degree of

Master of Science

in

Materials Science and Engineering

Stony Brook University

May 2014

Stony Brook University

The Graduate School

Wenbo Wang

We, the thesis committee for the above candidate for the

Master of Science degree, hereby recommend

acceptance of this thesis.

Dr. Gary Halada, Thesis Advisor, Professor
Department of Materials Science and Engineering

Dr. Dilip Gersappe, Professor
Department of Materials Science and Engineering

Dr.Balaji Raghothamachar, Doctor
Department of Materials Science and Engineering

This thesis is accepted by the Graduate School

Charles Taber
Dean of the Graduate School

Abstract of the Thesis

Molecular Modeling of the Interaction between Chitosan and Silver and Palladium

by

Wenbo Wang

Master of Science

in

Materials Science and Engineering

Stony Brook University

2014

The purpose of this research was to study the interaction between chitosan and metal surfaces at the atomic level in order to better understand the mechanism of formation of catalytic noble metal nanoparticle (where chitosan serves as a shaping or encapsulating agent).

In this study, Molecular dynamics (MD) simulation was employed to study chitosan adsorption on different Silver and Palladium crystallographic planes at the atomic level. Chitosan were formulated by molecular dynamics simulation named Materials Studio 6.0 using COMPASS force field. By calculated result of the solubility parameter δ, the length of chitosan was chosen 20 repeated units. Through MD simulation of chitosan chain, the result of the glass transition temperature of chitosan was similar to the experiment value as 476K.And the water content of chitosan was able to effect the glass transition temperature obviously as the water content increase that the glass transition temperature decrease. The interaction energy between chitosan and different metal surfaces indicates that the interaction of chitosan and silver (1 1 0) surfaces is stronger than that of (1 1 1) and (0 0 1) surface and the interaction of chitosan and palladium (1 1 0) surfaces is stronger than that of (1 1 1) and (0 0 1) surface. The concentration profiles show that hydrogen and amino groups of chitosan could form strong interactions with the surfaces of metal. The radial distribution function show that the probability of forming the nitrogen atoms

and metal on the surface have physical interactions. This study provides useful information in understanding the interfacial interaction mechanism at the atomistic scale for polymer and metal.

Table of Contents

List of Figures/Tables/Illustrations

Acknowledgments

I would like to sincerely tank my advisor Professor Gary Halada for giving me a chance to work with him. He really gave me a lot of help and guidance in my research. Since I was a beginner when I joined the project, he always encouraged me that I have done a good work. His encouragement and suggestion made me always feel confident in my research.

I would also thank Professor Dilip Gersappe for teaching me all the basic knowledge about Molecular Modeling and being my thesis committee members.

A special thanks to Dr.Lu, for helping me all the time during my research.

Finally, I thank my mom and my dad, for their love and concern for me at all times.

1. Introduction

1.1 Background

Chitosan has a number of perfectly natural properties, such as biocompatibility, nontoxicity, absorption, antibacterial property, and non-antigenicity. As an important chemical material, it has a broad range of applications in many fields, including biology, food industry and separation membrane. Great concern has been given, especially, on its applications in cornea repair and food preservation. Since the permeability affects the performance of the materials directly, it is very important and meaningful to study the permeability of chitosan material. To meet the permeability requirements for these materials, modifications of chitosan material, classified as physical and chemical, are necessary. Adding inorganic or organic mediums in the preparation of membrane plays a significant role in physical modification methods.

Many papers indicate that adding inorganic or organic mediums in the membrane would improve its permeable property, while the mechanism of this process remains unclear. The current data for the permeability are mainly obtained from experiment. However, the diffusion mechanism, interaction of polymers at a micro-level, and the information at nanolevel, such as the effect of the added mediums to the surrounded polymer chain [1, 2], is hard to gain directly. Therefore, a more effective and efficient method to duel with these problems is necessary.

Recently, molecular simulation has been widely applied in studying the membrane structure and diffusion mechanism of small molecules in it. By using this method, many studies have computed the diffusion coefficient of small molecules in amorphous polymers [3- 12]. In this study, molecular simulation was exploited to understand the gas diffusion property of chitosan membranes and chitosan composite membranes and explore the relationship between the membrane structure and its properties, for building foundation of the development of novel materials.

1.2Molecular Simulation

Molecular simulation is an experimental technique to get the structure and behavior of molecules or clusters by using computer and the atomic level can be expected to reach. Physical and chemical properties of the objective system can be obtained from computational simulation of the moving behavior and structure of the molecules in it [13]. Molecular simulation has important applications in learning materials from the microscopic view, for example, simulating their structures, calculating their properties, forecasting their behaviors, and testing experimental results. With the rapid development of Computer Technology (CT), molecular simulation has become a new research tool [14- 18] to describe material model in the larger and larger space scale and time scale (Fig. 1-1) and be more and more widely applied in chemical industry and material areas.

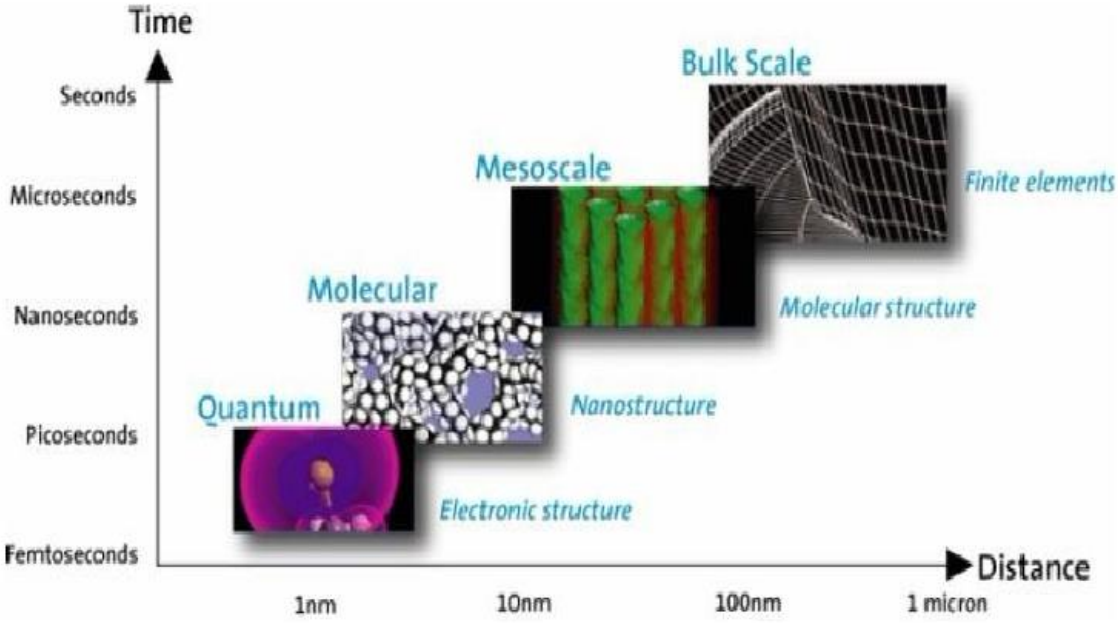

Figure 1-1 Relationship between molecular simulation, time scale and space scale

Molecular simulation is mainly divided into Quantum Mechanics (QM), Monte Carlo (MC), Molecular Mechanics (MM), and Molecular Dynamics (MD).

QM, based on the non-locality of electron, uses wave function to describe the behavior of electron. It can be employed to calculate different kinds of microscopic parameter in the system,

such as charge density, energy level, and electronic structure, and offer effective information of the three-dimensional structure and conformation. However, it is only suitable to the system with small number of atoms (teens to hundreds). MM is applied to simulate the dynamic properties of the system. It can describe the molecule structure with the bond length, bond angle and dihedral angle, and also illustrate the change of the energy in the system by using potential function. MD has been made use to simulate the dynamic properties of the system, like temperature, pressure, and diffusion coefficient. MC is a statistical method to deal with the problems with many factors. It simulate the system based on the 'random number', and its simulation result is the probability density.

Since the system in this study was large and the diffusion was one of the dynamic properties, MM, MC and MD were applied to discover the diffusion of permeation in the membrane material.

1.2.1 Molecular Mechanics Simulation

MM is also called force filed method, which is a quantum mechanics technology for structure optimization. It is essentially an energy minimization method to be applied to obtain the best structure of the system, which means minimizing the energy by changing the coordinate of the particle. Its principle is as following: since the inner stress in the molecule structure can reflect its relative potential energy, the minimum value of the system's potential energy can be reached by selecting the proper force field to calculate the potential energy of all kinds of possible conformation, adjusting the geometric structure of the molecule, and modifying the bond length, bond angle and dihedral angle of the molecule. The bond length, bond angle, dihedral angle and relevant force constant is called force field, in other word, force field is a simple mathematical expression of potential energy function.

1.2.1.1 Molecular Force Field

At the present, the force fields that used for the polymer system are UFF, CVFF, PCFF, Dreiding, AMBER, CFF, MM, CHARM, COMPASS, etc. The COMPASS is the most widely used among them [19].

COMPASS stands for Condensed-phase Optimized Molecular Potentials for Atomistic Simulation Studies. COMPASS represents the state-of-the-art force field technology. It is the first ab initio force field that enables accurate and simultaneous prediction of structural, conformational, vibrational, and thermo-physical properties for a broad range of molecules in isolation and in condensed phases[20,21]. It is also the first high quality force field that consolidates parameters for organic and inorganic materials previously found in different force fields. Its coverage includes the most common organics, inorganic small molecules, and polymers, and some metal ions, metal oxides and metals. Although different models are used for different systems, all of the parameters in COMPASS are derived in a consistent manner so that, in principle, one could study very different systems including interfaces and mixtures. (http://www.esi.umontreal.ca/accelrys/life/cerius46/compass/1_Introduction.fm.html) Since COMPASS can model the mixture of different systems, it was chosen as the force field in this study and its potential function is as following:

$$
\begin{aligned}
E_{pot} = & \sum_{b}[K_2(b-b_0)^2 + K_3(b-b_0)^3 + K_4(b-b_0)^4] \\
& + \sum_{\theta}[H_2(\theta-\theta_0)^2 + H_3(\theta-\theta_0)^3 + H_4(\theta-\theta_0)^4] \\
& + \sum_{\phi}\Big[V_1\big[1-\cos\big(\phi-\phi_1^0\big)\big] + V_2\big[1-\cos\big(2\phi-\phi_2^0\big)\big] \\
& \qquad + V_3\big[1-\cos\big(3\phi-\phi_3^0\big)\big]\Big] \\
& + \sum_{x} K_x x^2 + \sum_{b}\sum_{b} F_{bb}(b-b_0)(b-b_0) \\
& + \sum_{\theta}\sum_{\theta} F_{\theta\theta}(\theta-\theta_0)(\theta-\theta_0) + \sum_{b}\sum_{\theta} F_{b\theta}(b-b_0)(\theta-\theta_0)
\end{aligned}
$$

$$+\sum_{b}\sum_{\phi}(b-b_0)(V_1\cos\phi+V_2\cos2\phi+V_3\cos3\phi)$$
$$+\sum_{\theta}\sum_{\phi}(\theta-\theta_0)(V_1\cos\phi+V_2\cos2\phi+V_3\cos3\phi)$$
$$+\sum_{\phi}\sum_{\phi}(V_1\cos\phi+V_2\cos2\phi+V_3\cos3\phi)(V_1\cos\phi+V_2\cos2\phi+V_3\cos3\phi)$$
$$+\sum_{\phi}\sum_{\theta}\sum_{\theta'}K_{\phi\theta\theta'}\cos\phi(\theta-\theta_0)(\theta'-\theta_0')+\sum_{i>j}\frac{q_iq_j}{\varepsilon r_{ij}}$$
$$+\sum_{i>j}\left[\frac{A_{ij}}{r_{ij}^9}-\frac{B_{ij}}{r_{ij}^6}\right]$$

Where r, θ, ϕ, x represent covalent bond, bond angle, torsion angle, and dihedral angle respectively. K, H, F, V are force field parameters.

1.2.1.2 Energy Minimization

There are three energy minimization methods that are used in the molecule simulation: steepest-descent method, conjugated gradient method and Newton-Raphson method. Among all of the methods, steepest-descent method is the simplest one and approaches the minimum value quickly when the energy difference is large. Conjugated gradient method can be applied to large systems, but not suitable to the system with large energy difference. Newton-Raphson method converges more accurately and rapidly, however its computation cost is also huge. Thus, it is not applied to large system.

In this study, the Smart Minimizer in Material Studio was adopted to do energy minimization. This method combines all the advantages of the three methods listed above, and improves the speed and accuracy of the system structure optimization.

1.2.2 Monte Carlo Simulation

Monte Carlo method is a statistical experimental method that the macroscopic properties, only the equilibrium properties, of the system are computed from the large amount of microscopic states.

1.2.2.1 Basic Principle

For solving a certain problem, a proper stochastic model or process is build up based on some characteristics for this problem. The solution of the problem is equaled to the model parameter, like the probability of the event, or the expectation of a random variable. The results from several random sampling experiments are then analyzed statistically and the approximate solution can be obtained. There are mainly three steps for using Monte Carlo method to solve the problem: describing the probability model, realizing sampling from the known probability density, getting variety of estimations.

Theoretically, the Monte Carlo method can be used to calculate the statistical mean value. However, great deals of sample points are needed when dealing with some large systems, and the corresponding structure for many of these sample points are hard to appear due to the high energy. Besides, the integration for the structure is not easy to converge. Hence, it is rarely practical to use MC directly. Instead, the Metropolis's important sampling is usually used.

1.2.2.2 Metropolis Sampling

Metropolis method, which is first proposed by Metropolis, Rosenbluth, Teller, etc. in 1953, is the foundation of the computation of modern MC method. The main part of the Metropolis method is to build up the Markov chain for the system and let it meet the requirement for the important sampling. The Markov chain must satisfy the following two conditions:

Let $\left\{\overset{\mathrm{r}}{r_1^N}, \overset{\mathrm{r}}{r_2^N}, \ldots, \overset{\mathrm{r}}{r_m^N}, \overset{\mathrm{r}}{r_n^N}, \ldots\right\}$ be the finite set of all status of the system, then the status $\overset{\mathrm{r}}{r^N}$, generated from a random sample point, must be one of the status in the set.

The current selected sample point is only correlated to the last one point, and has nothing to do with the start point of sampling.

1.2.3 Molecular Dynamics Simulation

Molecular dynamics method can compute both the equilibrium properties and all kinds of dynamic properties. It can be used to describe the atomic actions, which means that computing the changes of each atom along time, after setting a potential function and initial velocities for all of the atoms in a certain system.

1.2.3.1 Basic Principle

Molecular dynamics considers Newton's second law of motion as its basic principle. In a given system, from the coordinates of each atom, the potential energy of the system can be calculated by potential function. The trajectories of atoms are determined by numerically solving the Newton's equations of motion for the system, where force between the atoms and their accelerations at different time are determined. By making use of statistics to analyzing the trajectories, macroscopic properties of the system (diffusion coefficient, glass-transition temperature, and etc.) are obtained.

1.2.3.2 Basic Steps of Molecular Dynamics Simulation

For a given object of study, its basic steps of molecular dynamics simulation are as Fig. 1-2.

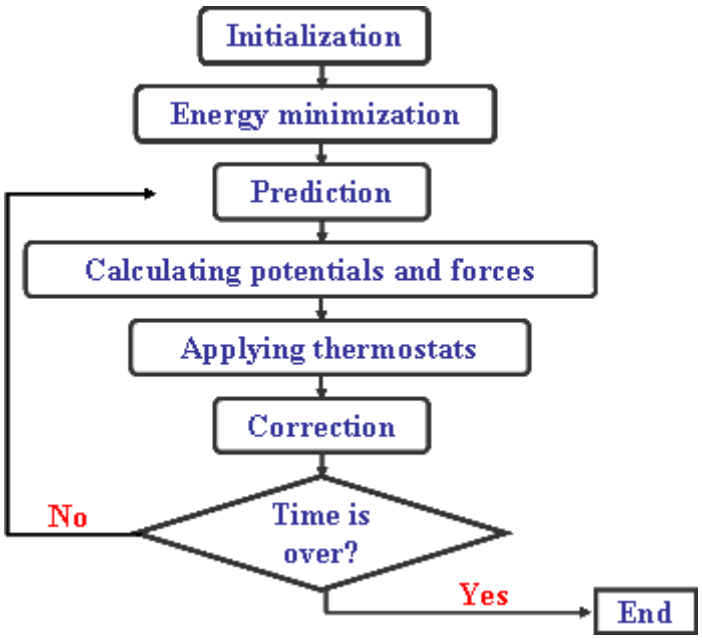

Figure 1-2 Basic steps of molecular dynamics simulation

1.2.3.3 Solving the Newton's Equations of Motion

In the computation of molecular dynamics, the velocity and location of the atoms are gotten by solving Newton's equations of motion. The commonly used methods are Beman algorithm [23] and Verlet algorithm [24]. Some other methods are Velocity-Verlet algorithm [25], Rahman algorithm [26], Leap-frog algorithm [27] and etc. In this study, the most convenient and accurate algorithm, Verlet algorithm, was employed.

1.2.4 Periodic Boundary Conditions

Molecular dynamics simulation is usually applied to simulate properties of large system. Due to the limitation of the computing power, in practical simulation, it is impossible to simulate an infinitely large system directly. More often, a cellular volume element that contains 100- 1000 atoms is chosen as the object of study. The reduction of the number of particles in the system will cause the finite-size effect, such that the force of the internal molecules is different from that of the surface ones, which is the surface effect. Because of this, there exists difference in the properties and behaviors between the simulated cellular system and the real system. To solve this

problem, the periodic boundary conditions are often adopted, since the real system is a network that consists of several identical small systems (Fig 1-3). The application of the periodic boundary condition extends the simulated cellular system to the real system. It seems that an approaching infinitely large volume is constructed to represent the macro system. Its mathematical expression is as (1-1)

$$\boldsymbol{A(\vec{x}) = A(\vec{x} + \vec{n}L)}, \qquad \boldsymbol{\vec{n} = (n_1, n_2, n_3)} \tag{1-1}$$

Where $A$is arbitrary observed value, n_1, n_2, n_3 are any integer, L is the length of the side of the cell, and $\vec{x}$ is the coordinates.

Periodic boundary conditions replicate the simulated unit cell completely infinite times. When a particle passes through one face of the unit cell, it reappears on the opposite face with the same velocity.

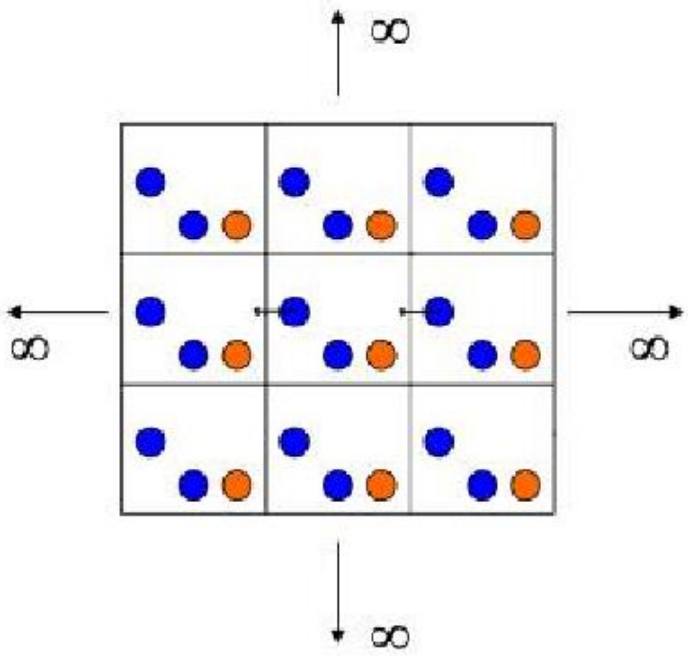

Figure 1-3 Periodic boundary conditions

2. Selection of Simulation Software, Parameters and Methods

2.1Introduction

Recently, molecular simulation technology plays more and more important role in the fields like chemistry and material science. With its rapid development, different kinds of simulation software have been brought out. To select the proper simulation software is the basement of the simulation work. Also, the selections of simulation parameters and the processing method for the simulation result are also significant to the accuracy of the experiment result. Therefore, it is necessary to determine the simulation software, simulation parameters and calculation method before doing the simulation.

2.2 Simulation Software

Materials Studio has been employed to do the simulation. It is developed and distributed by Accelrys at the year of 2000. It is a complete modeling and simulation environment designed to allow researchers in materials science and chemistry to predict and understand the relationships of a material's atomic and molecular structure with its properties and behavior. It contains tools useful for applications in Crystallization, Polymers and Classical Simulations, Quantum Mechanics and Catalysis, and Statistics.

Materials Studio includes many advanced simulation methods, such as Quantum Mechanics, Monte Carlo, Molecular Mechanics, and Molecular Dynamics. The components that were used in this study are Amorphous Cell, Discover, Forcite and Sorption.

2.2.1Amorphous Cell

Amorphous Cell develops an understanding of molecular properties and behavior, especially for liquids and amorphous polymers, with this versatile suite of computational tools. Predict and investigate properties such as cohesive energy density, equation-of-state behavior, chain packing and localized chain motions.

(http://accelrys.com/products/materials-studio/polymers-and-classical-simulation-software.html)

2.2.2Discover

Discover offers powerful atomistic simulation methods that can be applied to a wide range of molecules and materials. Discover is Materials Studio's simulation engine. It incorporates a broad spectrum of molecular mechanics and dynamics methodologies that have demonstrated applicability to molecular design. Using a carefully-derived force field as the foundation, minimum energy conformations, as well as families of structures and dynamics trajectories of molecular systems, can be computed with confidence. Comprehensive analysis features enable the extraction of pertinent results from the simulation.

2.2.3Forcite

Forcite is an advanced classical molecular mechanics tool, which allows fast energy calculations and reliable geometry optimization of molecules and periodic systems. Forcite is designed to work with a wide range of force fields. Currently, COMPASS, Dreiding, Universal Force Field, CVFF, and PCFF are supported, providing the opportunity to handle any chemical system. There are several choices of geometry optimization algorithms: Steepest descent, Quasi-Newton, Conjugate Gradient, ABNR, or the Smart algorithm.

2.2.4Sorption

Sorption provides a solution for the prediction of molecular adsorption in crystalline materials and on surfaces. Molecular adsorption into micro-porous structures such as zeolites, aluminophosphates, or polymers is crucial in numerous applications including air separation, hydrocarbon cracking, gas sensors, and ion exchange. Sorption provides a means of predicting fundamental properties, such as sorption isotherms (or loading curves) and Henry's constants, needed for investigating separations phenomena. In addition, modeling can be used to rationalize sorption properties in terms of molecular level processes.

2.3 Simulation Parameters

2.3.1Force Field

There are many kinds of force fields that are used in the MD simulation. In this study, COMPASS was selected based on the comparison of the simulated density of target material with the experimental data and the universality of the force field.

1) Suitability to chitosan

The structure model of chitosan was built up by the Visualizer in MS. Energy optimization and MD optimization was processed to the structure by COMPASS. The simulated density for chitosan was 1.34 g/cm^3. The density of chitosan was closed to 1.4 g/cm^3 shown on the literature [107], which illustrated that COMPASS was suitable to chitosan system

2) Suitability to silver and palladium

By using the space group of silica crystals and crystal parameter, the structure of silver and palladium were built. Energy optimization and MD optimization was processed to the structure by COMPASS

2.3.2 Cut-off Methods and Radius

In the dynamics calculation, the calculation of nonbonding interactions is time-consuming. The nonbonding forces include van der waals force and electrostatic force. To reduce the calculation cost, the potential energy was truncated without losing of accuracy. The commonly used methods are as following:

Direct cut-off, which means choosing radial cut-off radius directly. The cut-off radius r_c should be the point at which the potential energy approaches 0. To speed up the calculation, the cut-off distance r_c should be as short as possible.

Applying switching function. In some accurate calculation, the potential energy at the cut-off distance is not 0. If setting it to 0 directly, the energy would be not continuous, and become a

fake low potential energy point. To solve this problem, switching function is usually used. It satisfies the characteristics: when atoms' distance r is less than the switching variable r_s, the function obtains the value 1; when r is greater than r_s and less than r_c, the function approaches 0; when r is greater than r_c, the function equals 0. The introduced switching function makes the cut- off more precise. Figure 2-1 shows the calculation of the cut-off distance.

Using constant moving. This method is used to reduce the potential energy surface faults. It is to move the potential function by a given constant, to let the potential function be 0 at r_c.

In this study, the simplest and most directly method, Atom based cutoffs, is used to calculate the van der waals force. And using the most feasible method, Ewald summation method, calculates the electrostatic force, with the cut-off distance being 1.25 nm. The simulated density of chitosan is 1.338 g/cm^3, which is similar with the experimental value 1.4 g/cm^3.

2.3.3 Time Step

In the calculations of molecular dynamics, the time step has essential effect to the calculation cost and precision. Within a certain time scope, the less the time step is, the less the error would be and the longer the time would be cost; the larger the time steps it, the less time cost in practice, however, the error would be very huge due to the unstable system caused by the particles with high energy. Usually, to reduce the error in simulation computation, the time step should be small, and should be less than the one tenth of the shortest period of motion. In practice, the selection of the time steps is usually based on the simulation experience. In this study, the time step is selected as 0.5-1 fs.

2.3.4Temperature Control Method

The system temperature is directly related to the kinetic energy obtained from the atom velocity and is an important indicator reflecting the thermodynamic state of the system. The relationship of temperature and atom velocity can be expressed by Maxwell-Boltzmann equation:

$$f(v) = \left(\frac{m}{2\pi k_b T}\right)^{\frac{2}{3}} \exp\left(-\frac{mv^2}{2k_b T}\right) 4\pi v^2 \quad (2\text{-}1)$$

Temperature is a thermodynamic variable and is only meaningful when the system is balanced. It is related to the system's average kinetic energy through energy equipartition. To study a certain property of the system, the temperature is usually controlled on a fixed value. Therefore, controlling the system temperature and maintaining it around a constant value or to be equal to the outside temperature is of great meaning to the molecular dynamics simulation. The temperature control methods in Materials Studio include Direct velocity sealing, Berendsen [65], Nose-Hoove [66, 67], and Andersen [68].

2.4 Computing Method of the Main Physical Parameters

2.4.1Glass Transition Temperature

The glass transition temperature of a polymer is often calculated through simulating the specific volume versus temperature plot of the polymer system. The NPT dynamics simulation is processed in optimal balancing system. The relationship of the specific volume and temperature of the system is obtained by heating up gradually and processing NPT-MD simulation at different temperatures. Two straight lines are fitted for each part of the data and then the intersection point would be the glass transition temperature. (As shown in Figure 2-2) In this study, this method is used to calculate the glass transition temperature.

2.4.2Activity of Polymer Molecular Chain

The activity of polymer molecular chai is usually expressed by its mean square displacement. The mean square displacement (MSD) is defined as:

$$MSD = \langle \left(r_i(t) - r_i(0)\right)^2 \rangle \quad (2\text{-}2)$$

where, $r_i(t)$ and $r_i(0)$ are the end and starting positions of the centroid of the particle i at time t. $\langle\ \rangle$ indicates the average of all molecules and time points. The activity of chain is determined by

the slope of MSD – t curve, and the larger the slope is, the more activity it is. This method is simple and the activity can be easily obtained from calculating the changes of the particle's position. In this way, it was used to describe the activity of the chains in this study.

2.4.3Interaction Energy

ΔE is used to represent the interaction energy or binding energy of polymer-inorganic material or polymer-polymer.

$$\Delta \boldsymbol{E} = \boldsymbol{E_{12}} - \boldsymbol{E_1} - \boldsymbol{E_2} \tag{2-3}$$

where E_{12} means the total energy of polymer-inorganic material or polymer-polymer system, and E_1 and E_2 are the individual energy of polymer and inorganic, or polymer 1 and polymer 2, respectively. The absolute value of ΔE determines its magnitude. If ΔE is negative, then the system energy decreases due to the bond of the two material and the system tends to be stable; If ΔE is positive, then the system energy increases due to the bond of the two material and the system tends to be unstable

2.5 Summary

In this chapter, the software and related module adopted in the molecular simulation were selected and explained in detail. Also, the computing method of the basic parameters and main properties, like interaction energy, activity of molecular chain and etc., was determined.

1. The modules in the MS that were used in this study are Amorphous Cell, Discover, Forcite and Sorption modules.

2. The COMPASS force field was employed. The potential energy was cut-off using atom based cutoffs method, and the cutoff radius is 1.25 nm. The Andersen method is selected as the temperature control method.

3. According to the literatures and experience, the glass transition temperature of a system was calculated through simulating the specific volume versus temperature plot of the polymer system. And the MSD curve was used to represent the activity of the polymer molecular chain.

3. Molecular modeling of the membrane of chitosan

3.1 Introduction

Our long term goals are to use a combined analytical and modeling approach, integrated with optimization of synthesis and electrochemical testing methodologies, to develop a comprehensive understanding of the noble metal/polysaccharide interface. In particular, this work will focus on improving our understanding of a newly developed process for electrochemically-driven synthesis of silver and palladium nanoparticles in a chitosan matrix, a process which is extremely rapid, occurs at room temperature in simple solutions and which preliminary data has shown to produce surfaces of high durability under atmospheric and service conditions which can serve as catalysts for key reactions in fuel cells (Figure.3-1). Models can be made based on chitosan molecules with varying degrees of deacetylation to provide information on the role of surface sorption sites for metal ions in the process of nanoparticle formation.

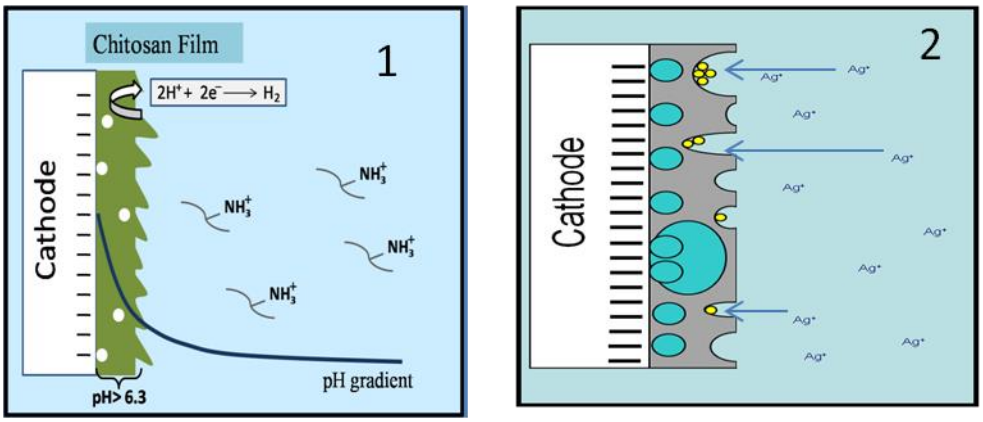

Figure 3-1 ***Two stage process for electrochemically-driven formation of silver nanoparticles on a deposited chitosan surface***

In particular, this work will focus on improving our understanding of a newly developed process for electrochemically-driven synthesis of silver and palladium nanoparticles in a chitosan matrix, a process which is extremely rapid, occurs at room temperature in simple solutions and which preliminary data has shown to produce surfaces of high durability under atmospheric and service conditions which can serve as catalysts for key reactions in fuel cells (Figure.3-1). Models can be made based on chitosan molecules with varying degrees of deacetylation to provide

information on the role of surface sorption sites for metal ions in the process of nanoparticle formation.

3.2 Model construction and minimized

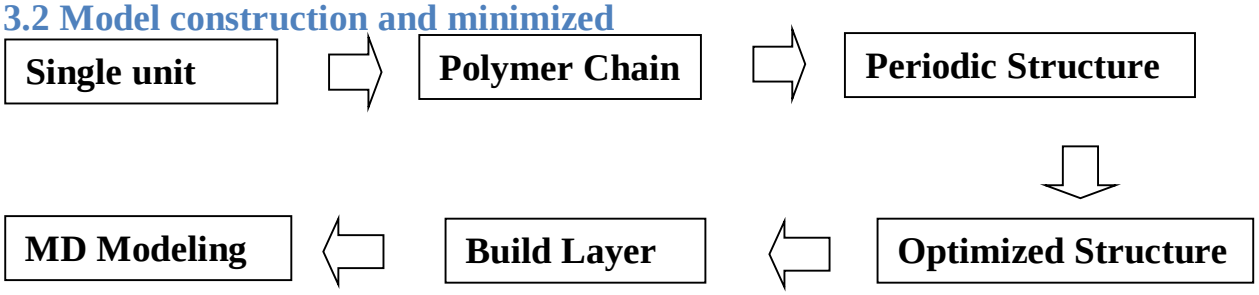

Figure 3-2 Basic process of model construction

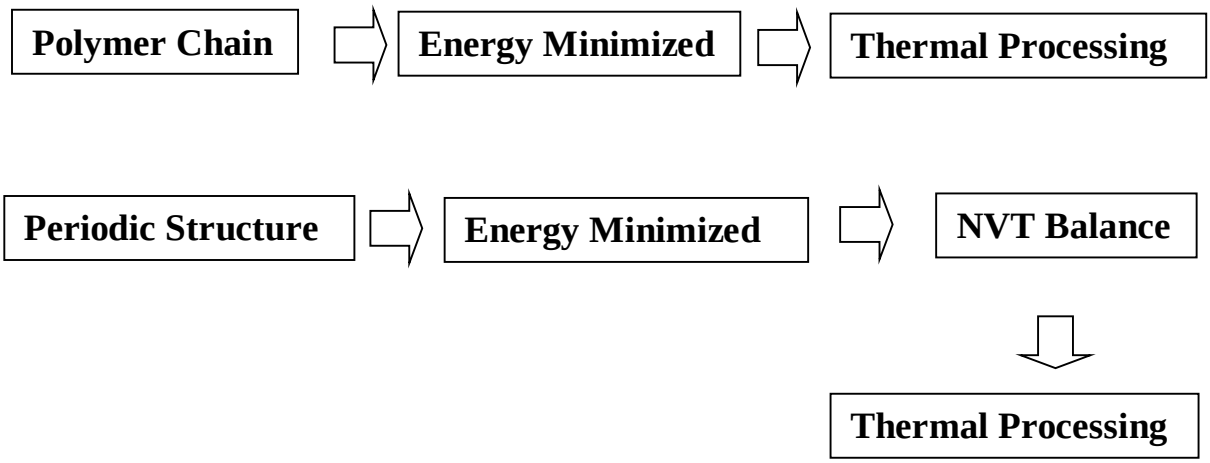

Figure 3-3 Basic process of model optimization

3.3 Chitosan model

The repeat unit of chitosan chain was constructed by means of Materials Studio using the Visualizer as Fig. 3-4.

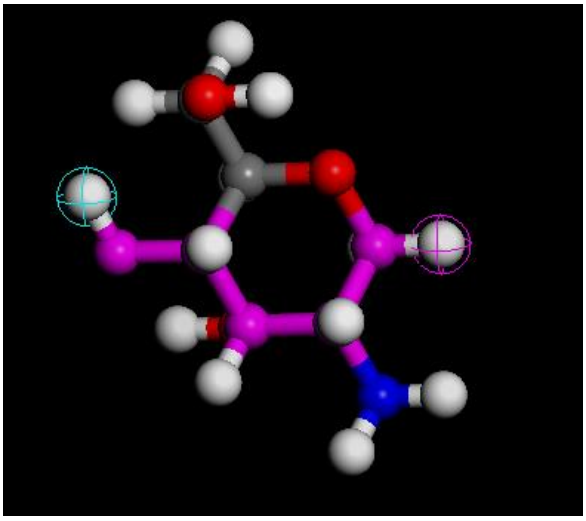

Figure 3-4 Repeat unit of Chitosan

Selected the head and the tail of the repeat unit as showed in Fig. 3-4, the blue circle represents the head and the red circle represents the tail. The chitosan chain was constructed by the polymer builder using the repeat units. In this simulation work, the length of chitosan chain was determined by calculating the solubility parameter δ according to Eq. (3-1):

$$\boldsymbol{\delta = \sqrt{CSD} = \sqrt{\frac{E_{coh}}{V}}} \tag{3-1}$$

Where CSD represents cohesive energy density. E_{coh} represents the cohesive energy and V is the volume of polymer. To reduce the statistical error, the parallel experiments were conducted using for each system investigated. While for every system, five simulations have been conducted. Computed values of δ are plotted vs repeating units of CS (up to 100 monomer units) in Fig.3-5. It is observed that, beyond 20 monomer units, the δ values did not vary much. Almost a similar dependency was observed by Qiang et al., [69] wherein it was found that for Chitosan interaction with Fe_3O_4, 20 repeating units were sufficient to perform the simulation. When the repeating unit reaches 20, δ approached a constant value and was close to the experimental data (10.6 ±0.8) [], therefore in this work, the length of chitosan chain was choose to be 20. The 3D structure of chitosan chain (20 units) was shown in Fig.3-6.

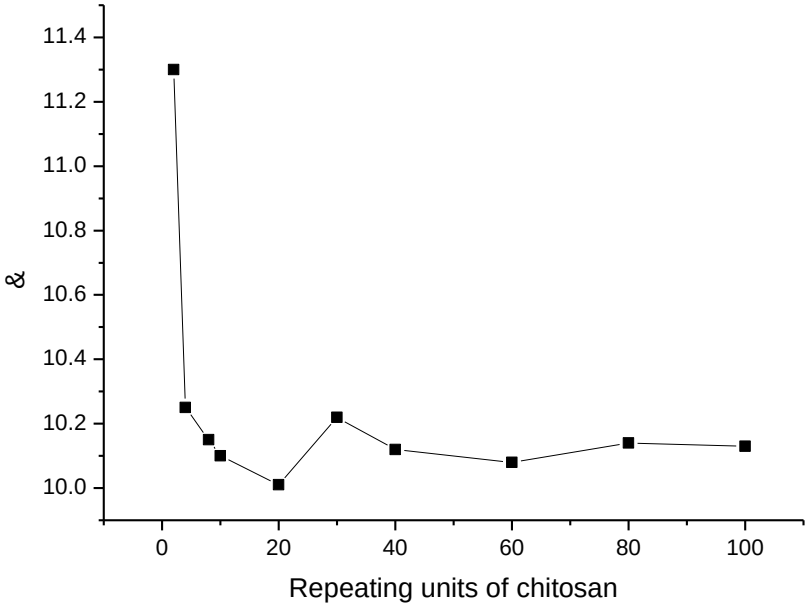

Figure 3-5 The solubility parameter depend on the number of repeating units

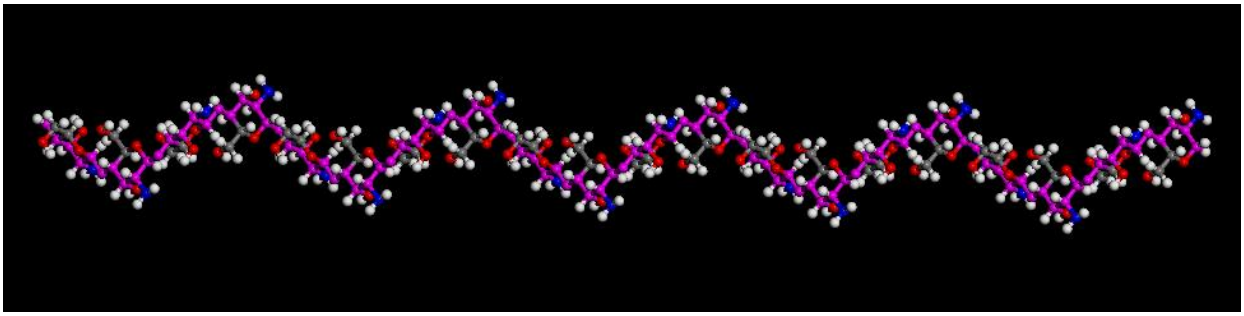

Figure 3-6 The 3D model of the chitosan chain (20 monomers). Carbon: gray; hydrogen: white; nitrogen: blue; oxygen: red.

The chitosan molecule was optimized by the steepest descent and conjugate gradient method. During the procedure of structure optimization, the maximum number for the minimization was 10,000. To obtain an energy-minimized state, the chitosan structure was annealed by performing dynamics simulations for 200 ps at each temperature, which increased from 298 K to 598 K and then decreased to 298 K with a step of 50 K. The simulations have performed with the time step of 1 fs at NVT ensemble. The optimized structure was shown in Fig.3-7.

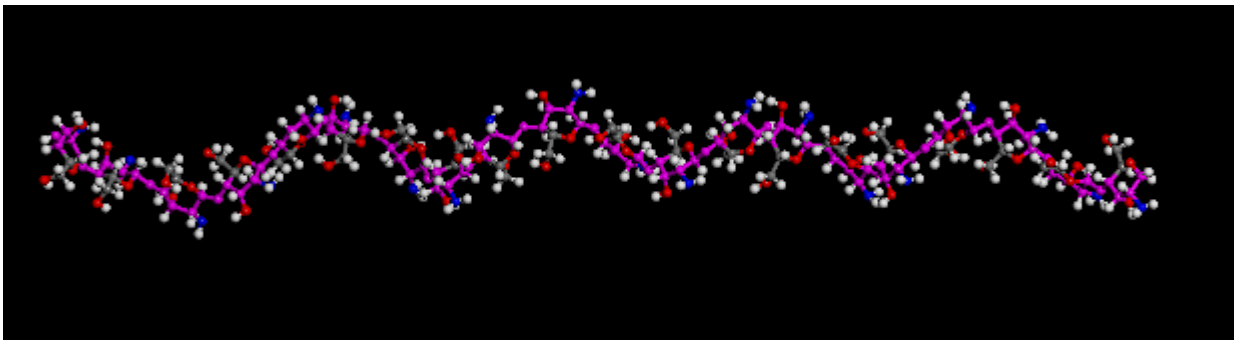

Figure 3-7 The optimized structure of the chitosan chain (20 monomers). Carbon: gray; hydrogen: white; nitrogen: blue; oxygen: red.

The chitosan chain which has 3D periodic structure was construct by the Amorphous Cell Module and was minimized by the steepest descent and conjugate gradient method. During the procedure of structure optimization, the maximum number for the minimization was 10,000. The optimized structure was shown in Fig.3-8.

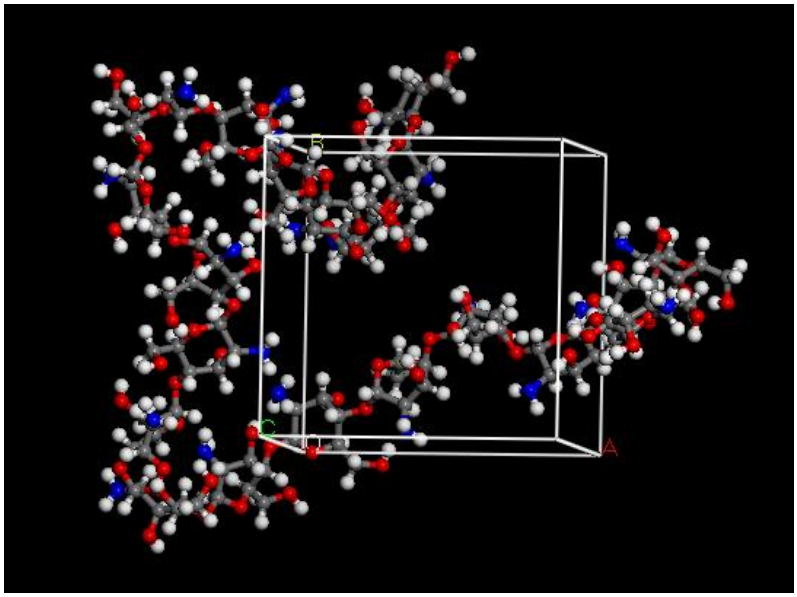

Figure 3-8 The optimized periodic structure of the chitosan chain (20 monomers). Carbon: gray; hydrogen: white;

3.4 The glass transition temperature of Chitosan

The glass transition temperatures (Tg) are related to the physical stability of an amorphous formulation and determinate the field of the materials be able to apply. Therefore, Tg has a significant value to research the chitosan. Below the Tg, pharmaceutically active materials

should be stable due to high viscosity. The structural relaxation time of a system slows dramatically at the Tg, and thus, the molecular mobility becomes extremely reduced.

In this work, these periodic cells were run MD simulation under isobaric isothermal conditions (NPT ensemble) at the temperature range between 348K and 548K and took each 20k as one step. At each step, an NPT MD run was carried out for 200 ps, where 150 ps allows for equilibration at the particular temperature and the last 50ps is used for data sampling. The final configuration of each individual 200 ps run served as the starting structure for the subsequent one. For the last 50 ps, at every picosecond the specific density (ρ_{spec}) was sampled, and the average value (over these 50 data points) was taken as the result. V_{spec} can subsequently be calculated via 1/ ρ_{spec}, and these specific volumes were plotted vs temperature (Figure 3-9).

The result was calculated from the plot by the turning point, which is between 476k and 489K. This result was similar to the result which is 476k by the method of DSC and DMA by Sakarui. It mean that the simulation and optimized process was property and the model was quite similar to the real one which proved the Molecular Dynamic Modeling is able to calculate the Tg.

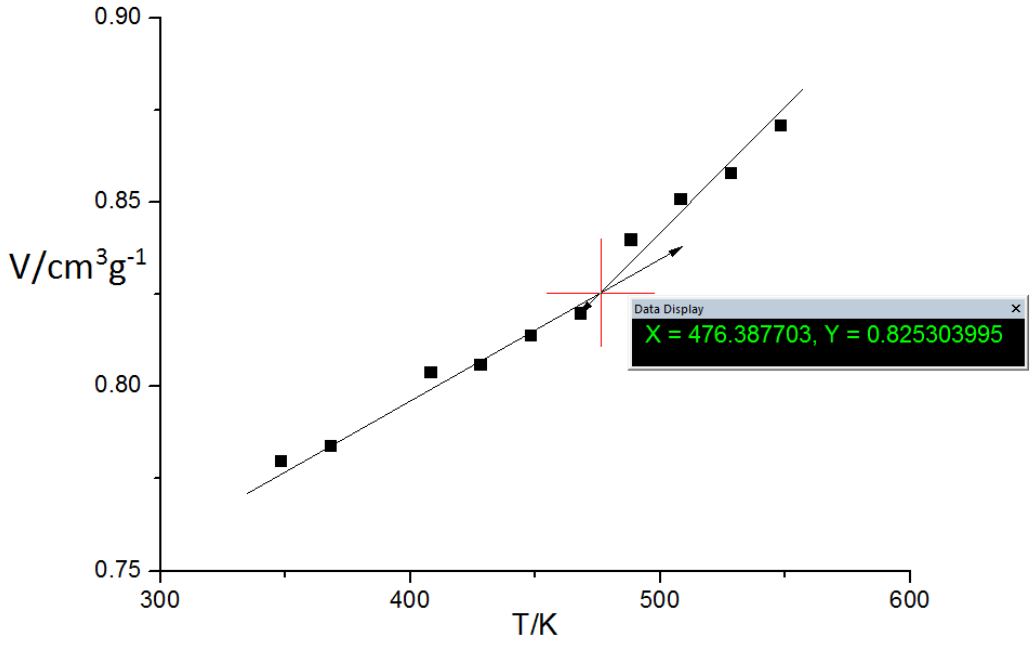

Figure 3-9 ***Specific volume of NPT dynamics versus temperature for CS***

3.5 The effect of water content of chitosan

The models of different water content of chitosan chain were built whose water content were 10%, 30% and 50% respectively as shown in the Fig.3-10. These 3D periodic structures were minimized under the same condition as mentioned in section 3.3.

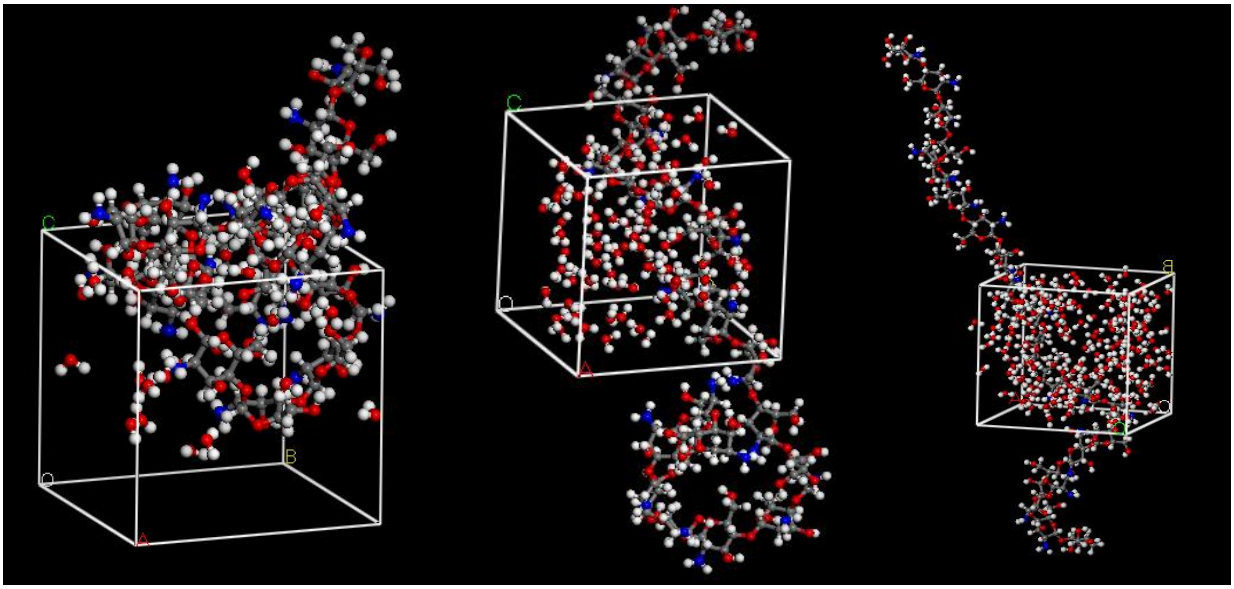

Figure 3-10 ***the different water content of the chitosan in 3D peroidic structure (a)10% (b) 30%(c)50%***

Table 3-1 ***Tg of CS membranes with different water content***

Water content (%)	0	10	30	50
Tg (K)	476	372	294	238

Table. 3-1 is glass transition temperatures of different water content of chitosan. As the table shown, when the water content is increasing, the glass transition temperature is decreasing. Compared to the chitosan with 0% water, Tg dropped to 372K. The reason is probably because

as the water content increased, the strong polarity between the water molecules and the chitosan which cause the chitosan developed to high-elasticity, however the chitosan was glass state in room temperature. What is more, there were strong interactions between the water molecules and the chitosan, the existence of the water molecules decreased the interaction among the chitosan chain and loosed the structure of the chitosan chain which caused the movement of the chitosan chain easier. Finally, the glass transition temperature was decreased.

4. Atomic-scale interactions of the interface between chitosan and Ag

4.1 Ag model

In this study, the initial coordinates of Ag were taken from the crystallography open database. The (1 1 1), (1 1 0) and (0 0 1) surfaces of Ag were chosen to study the interaction with chitosan, because they were the dominant surfaces observed in experiments. The surfaces of Ag were built by cleaving the crystal along the crystallographic planes. The dimensions of the Ag surfaces were as follows: Ag (1 1 1), 17.33 Å×20.22 Å×7.03 Å (a×b×c), α = β = 90◦, γ = 120◦; Ag (1 1 0), 16.34 Å ×14.44 Å ×10.11 Å, α = β = γ = 90◦; Ag (0 0 1), 17.33 Å×17.33Å×14.30 Å, α = β = γ = 90◦; (see Fig. 4-1). The minimization process was completed by the steepest descent method with the convergence of 1000kcal/mol and the conjugate gradient method with the convergence of 10 kcal/mol.

4.2 Interface model

The optimized chitosan chain was added onto the built Ag surfaces, and then the "vacuum slab" with the height of 10Å was put upon the chitosan–Ag system with 3D periodic boundary conditions. The initialization model of the Ag surface with the chitosan was shown in Fig. 4-2. The surfaces of Ag were fixed before simulations. The MD simulations of the adsorption of chitosan on Ag surface were studied in the canonical ensemble (NVT) at 298 K. The temperature of the systems was kept through the Andersen method. The time step was 1.0 fs and the dynamics balance time was 200.0 ps. And the whole MD simulation was performed under the same conditions to record the trajectory of all the atoms in the system. After reaching equilibrium state, the binding energy between the chitosan chain and the Ag surfaces were calculated to evaluate the interfacial interactions. The concentration profiles of the atoms (in the oxygen and amino groups of the chitosan) and the atoms (in the chitosan backbone) were used to examine the activity of groups and backbone of the chitosan during the adsorption process. The

radial distribution function (RDF) of different atoms could be used to understand the interaction of chitosan/Ag on the atom scale.

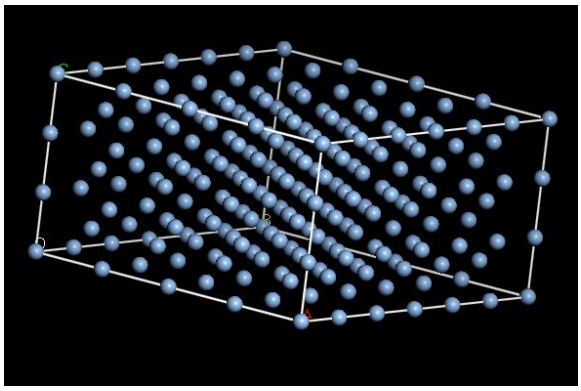

Figure a

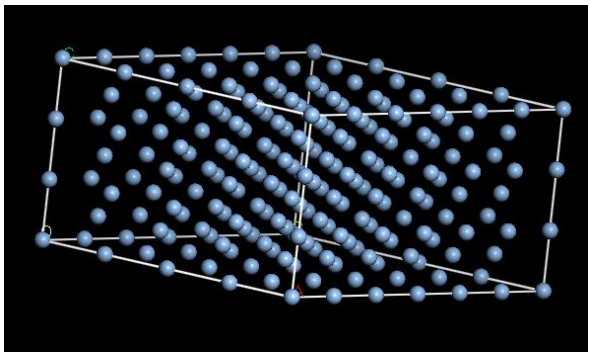

Figure b

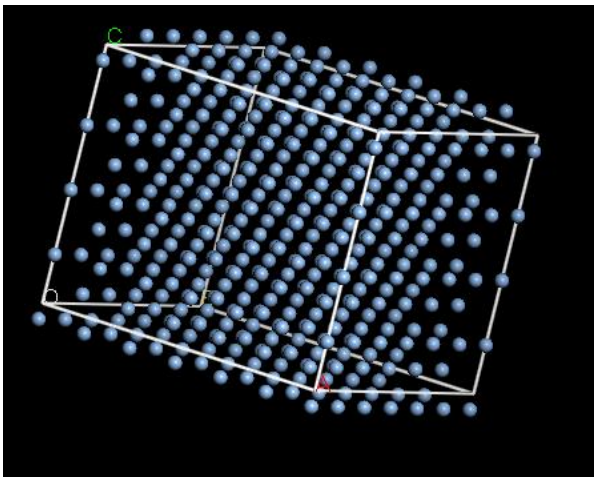

Figure c

Figure 4-1 the model of the Ag (1 1 1), (1 1 0) and (0 0 1) surfaces as Figure a, b, and c

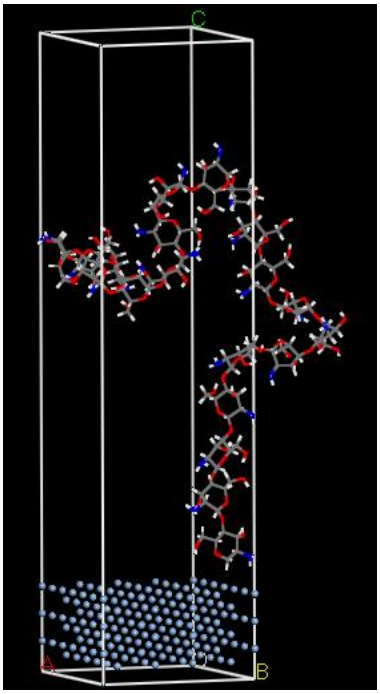

Figure 4-2 the interface between chitosan and Ag surface

4.3 Certification of the balance of the system

When study the properties of the system, the balance of the system is the fundamental problem to make sure. All the factors as temperature, density, energy are able to help to judgment the balance of the system.

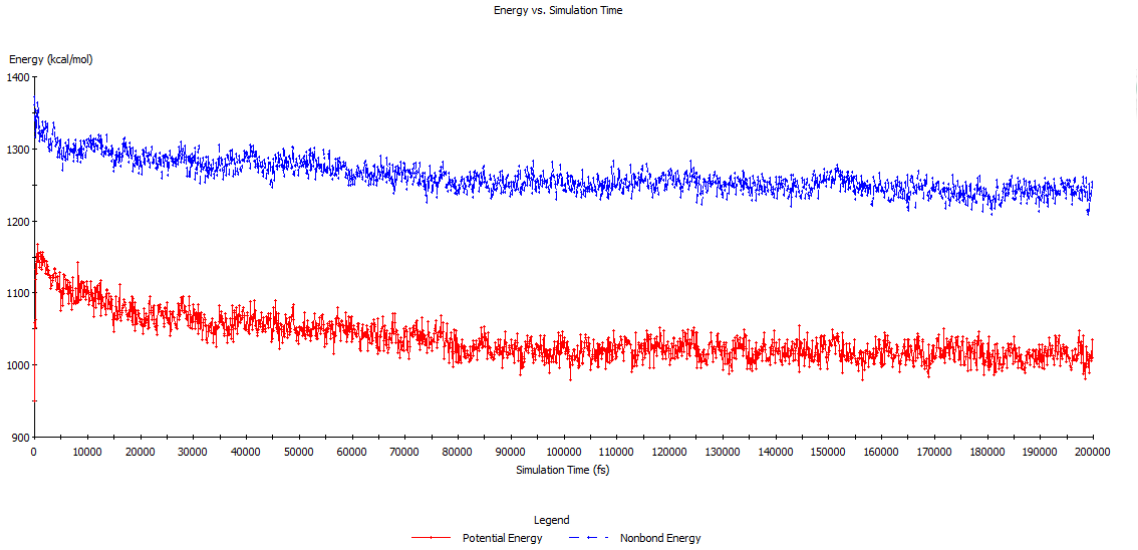

Figure 4-3 Energy fluctuation properties of Chitosan

In this work, the most usual method is used to test the balance which is using the temperature and energy. When the system energy was stable at the certain range and the temperature was change slightly during the set value, the system approached to balance condition. The curve of the energy change and the temperature change were shown in the Fig.4-3 and Fig.4-4.

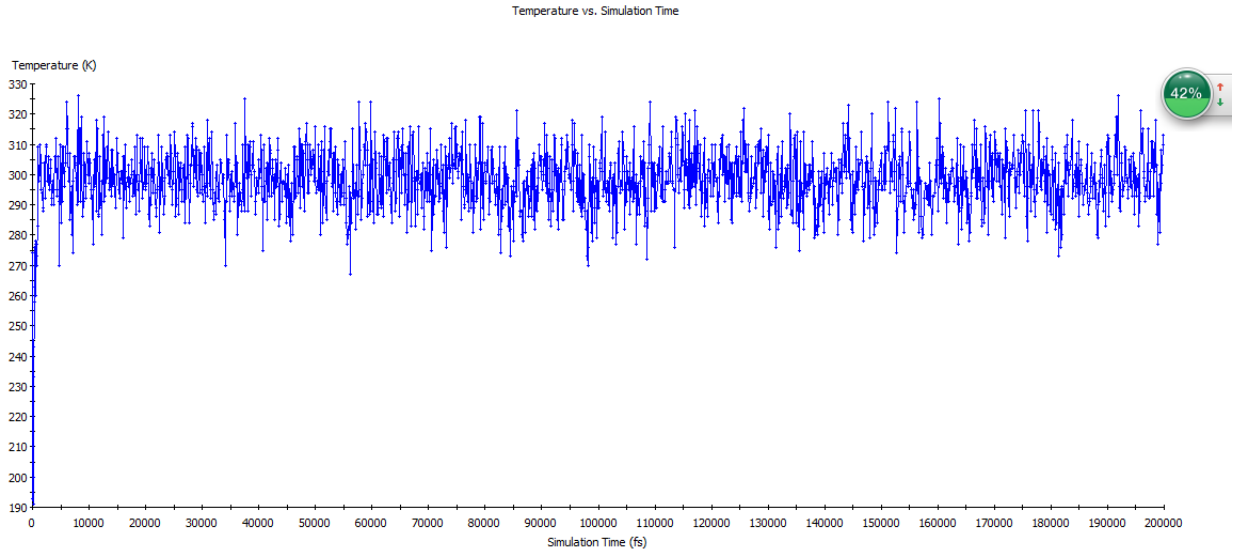

Figure 4-4 ***Temperature fluctuation properties of Chitosan***

4.4 Result and discussion

4.4.1 The interaction energy between chitosan and Ag

The interaction energy (E_i) reflected the interfacial compatibility and interaction. E_i between Ag and chitosan could be calculated by the following equation:

$$\boldsymbol{E_i = \frac{E_{CS} + E_{Ag} - E_{AgCS}}{S}} \quad (4\text{-}1)$$

Where E_{total} represents for the energy of Ag with chitosan after MD simulation, E_{Ag} is the energy of the Ag by removing the chitosan and E_{CS} is the energy of the chitosan chain after removing the Ag surface. S denotes the area of the Ag surface. The greater value of E_i implied stronger interaction, and more compatibility of the two components.

Table 4-1 presented the interaction energy of chitosan/Ag. It can be found that the value of E_i between chitosan and (1 1 0) surface was larger than that of the other surface. Therefore, the interaction between chitosan and (1 1 0) surface was greater than those of (1 1 1) and (0 0 1) surfaces, the interface interactions between chitosan/ (1 1 0) surface and chitosan/ (0 0 1) surface were very similar. Moreover, the surface free energy was nearly equal between (1 1 0) and (0 0 1) surfaces and they had similar surface structures. Therefore, we choose (1 1 1) and

(1 1 0) surfaces for the following study.

Table 4-1 the interaction energy between different Ag surfaces and Chitosan

Ag surface	Area($Å^2$)	E_{total}(kcal mol^{-1})	E_{CS}(kcalmol^{-1})	E_{Ag}(kcal mol^{-1})	E_i(kcal mol^{-1})
(1 1 1)	350.41	3311.28	1032.06	4287.57	5.731
(1 1 0)	235.95	3330.36	1051.27	4160.83	7.975
(0 0 1)	300.33	7815.68	8840.02	1073.14	6.986

4.4.2 The chain behavior of chitosan on Ag surface

Between chitosan and inorganic surface, there might be some physical and chemical interactions after adsorption. These interactions might lead to the configuration changes of chitosan and the changes of molecular models were able to observe by Molecular Dynamics simulation on both before and after adsorption. In this work, all the chitosan of different interfaces had the same initial configuration (see Fig.4-5(a)). The structures of the chitosan on (1 1 1) and (1 1 0) surfaces after MD simulation were shown in the Fig.4-5 and Fig.4-6. It could be seen that chitosan chain before simulation was the helical conformation and loosely stretched. And the hydrogen and amino groups in both sides of the chitosan chain. After MD simulation, the chain was trend to move to the Ag surface. The stretched chain was trend to huddle up.

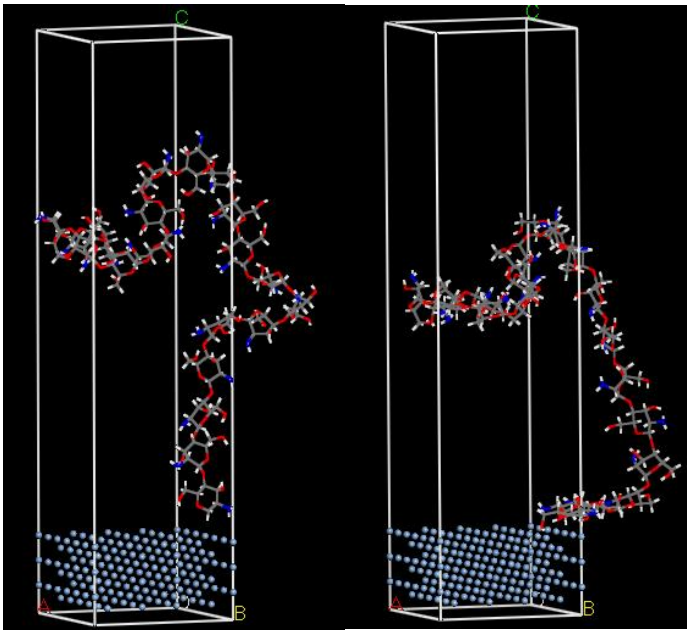

Figure a *Figure b*

Figure 4-5 The configuration of chitosan chain on Ag(1 1 0) surface(a)before MD simulation (b) after MD simulation

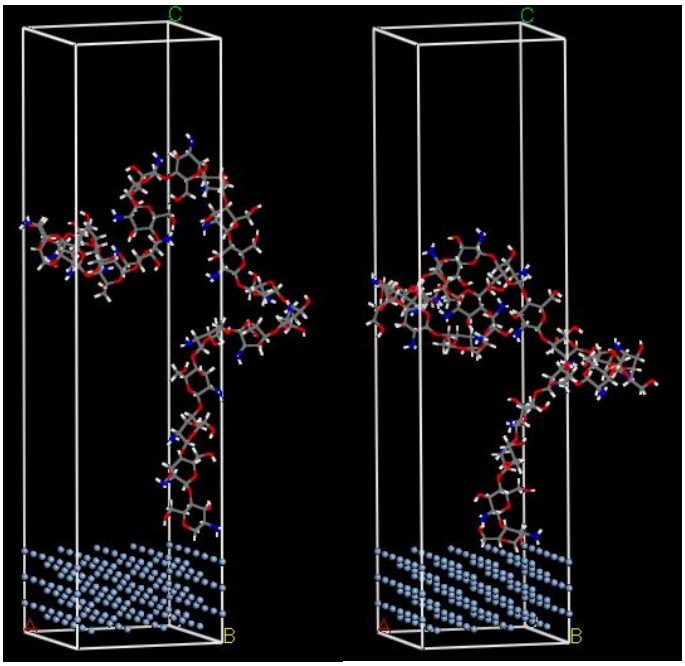

Figure a *Figure b*

Figure 4-6 the configuration of chitosan chain on Ag(1 1 1) surface(a)before MD simulation (b) after MD simulation

4.4.3 The concentration profile

The concentration profile was a function of the positions along the axes of the Ag surface and a distribution of the specific atom or group in the polymer. In this work, the concentration profile of hydrogen, oxygen, nitrogen atoms on the chitosan was choose along the axis normal to Ag surface. Firstly, the concentration profile if hydrogen atoms from the hydrogen and amino groups on the chitosan chain on the different surfaces. Before the MD simulation, the concentration profile was located in the range of 35-50 Å as shown in Fig.4-7. However, after the MD simulation, the other peak of the concentration profiles of hydrogen atoms on (1 1 1) surface and (1 1 0) were observed in the range of 10-12 Å. This was a very close distance between hydrogen atoms and Ag surfaces which might lead to the interaction. The strongest interaction was occurred in the closest distance which is the location of first peak. And the normalized are was used to compare the concentration distribution of the atom which have the closer distance on the surface. From the Fig.4-8(a) and Fig.4-9(a), the first peak of chitosan/ (111) surface was located in 12 Å; and the first peak of chitosan/ (110) surface was also located in 12 Å. Then, the normalized area of (111) which was obviously bigger than that of (110). This means there were more hydrogen atoms on the (111) surface in the closest distance than on the (110) surface. Therefore, there might be stronger interaction of hydrogen atoms/ (111) surface than hydrogen atoms/ (110) surface.

The concentration of oxygen atoms that belong to the hydrogen group of chitosan on the different surfaces were studied as shown inFig.4-8(b) and Fig.4-9(b). Before the MD simulation, the concentration profile was located in the range of 30-50 Å as shown in Fig.4-7. However, from the concentration profiles of hydrogen atoms on (1 1 1) surface and (1 1 0) after the MD simulation, the first peak of profiles were located in 11 Å. And the normalized area of (111) which was also bigger compare to the area of (110). Therefore, there were more oxygen atoms of hydrogen groups on the (111) surface in the closest distance.

Fig.4-8(c) and Fig.4-9(c) showed the concentration profiles of nitrogen atoms on chitosan/ (111) surface and chitosan/ (110) surface. And the normalized area of the first peak of (110) which was also bigger compare to the area of (111). Therefore, there were more oxygen atoms of hydrogen groups on the (110) surface in the closest distance.

The concentration profiles of carbon, oxygen and hydrogen atoms from the chitosan backbone on the different surfaces were shown in Fig.4-10, Fig. 4-11and Fig. 4-12. Compared with the atoms of hydrogen and amino groups on the chitosan chain, the atoms from backbone had a longer distance from the Ag surface. It means that the interaction between chitosan and Ag might mainly come from the groups of chitosan.

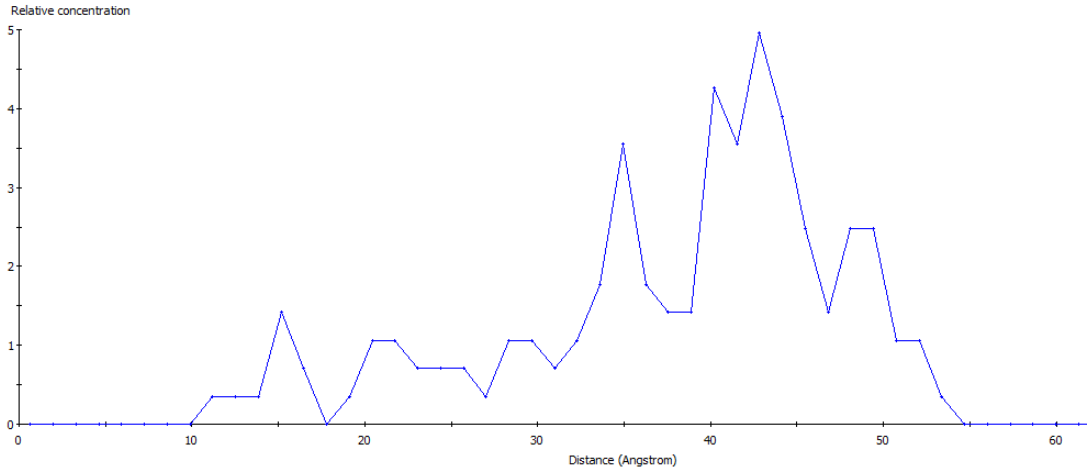

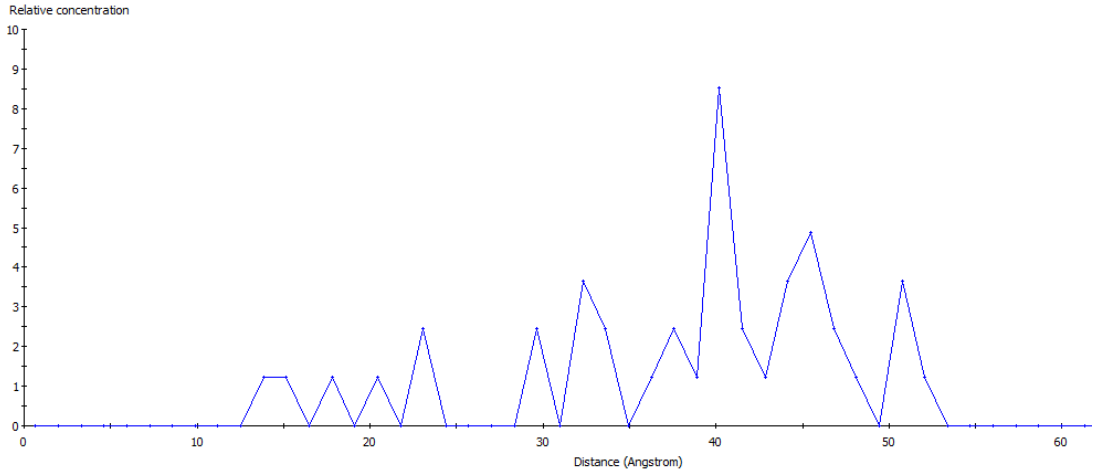

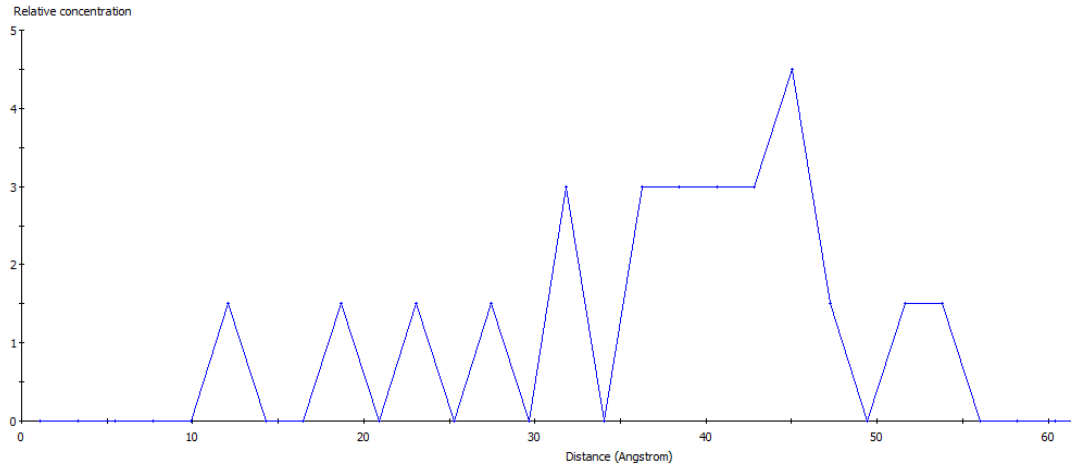

Figure 4-7 ***Concentration profiles of different atoms of groups on Ag surface: (a) hydrogen, (b) oxygen and (c) nitrogen atoms before the MD calculation***

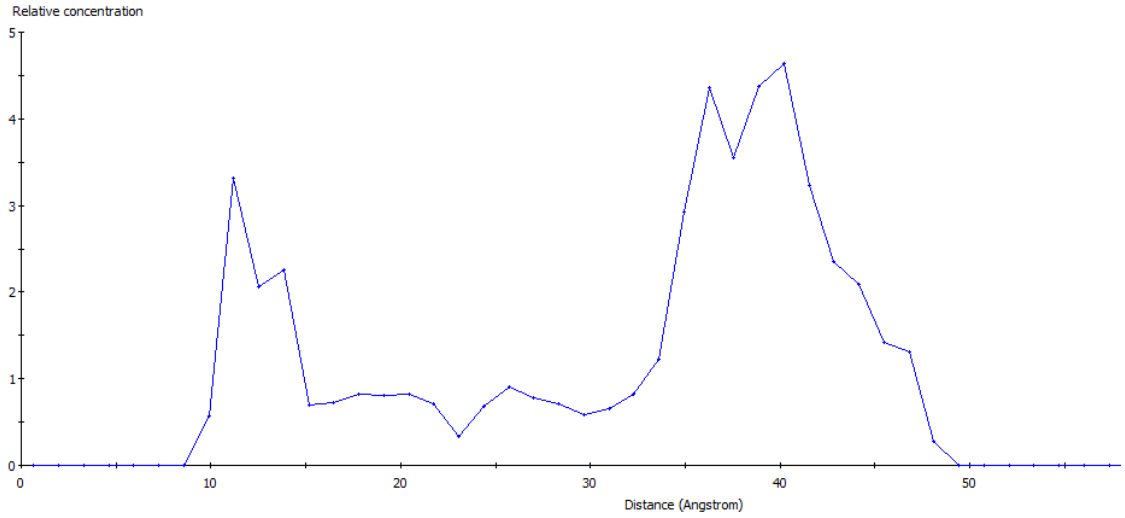

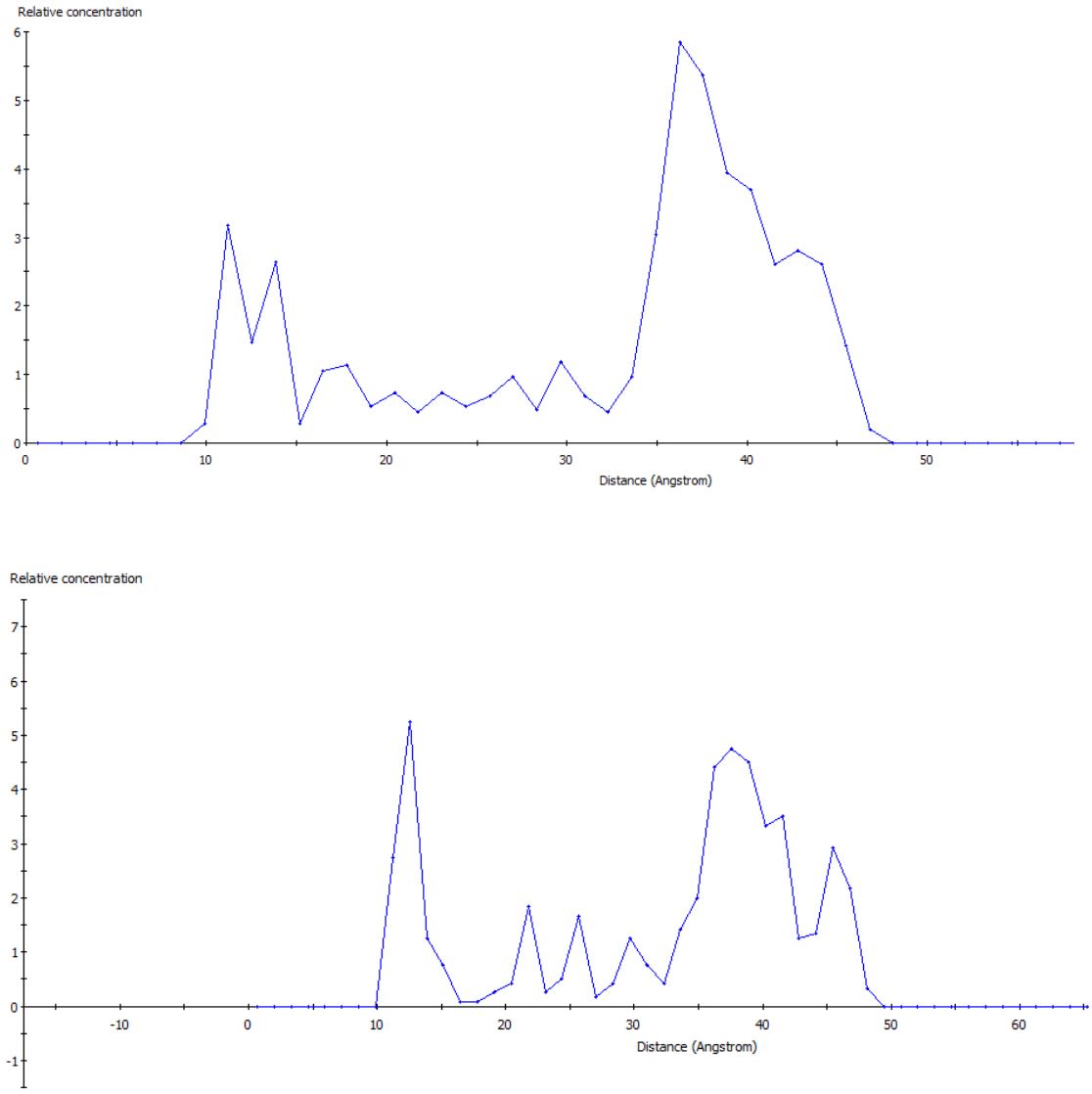

Figure 4-8 ***Concentration profiles of different atoms of groups on Ag (111)surface: (a) hydrogen, (b) oxygen and (c) nitrogen atoms after the MD calculation***

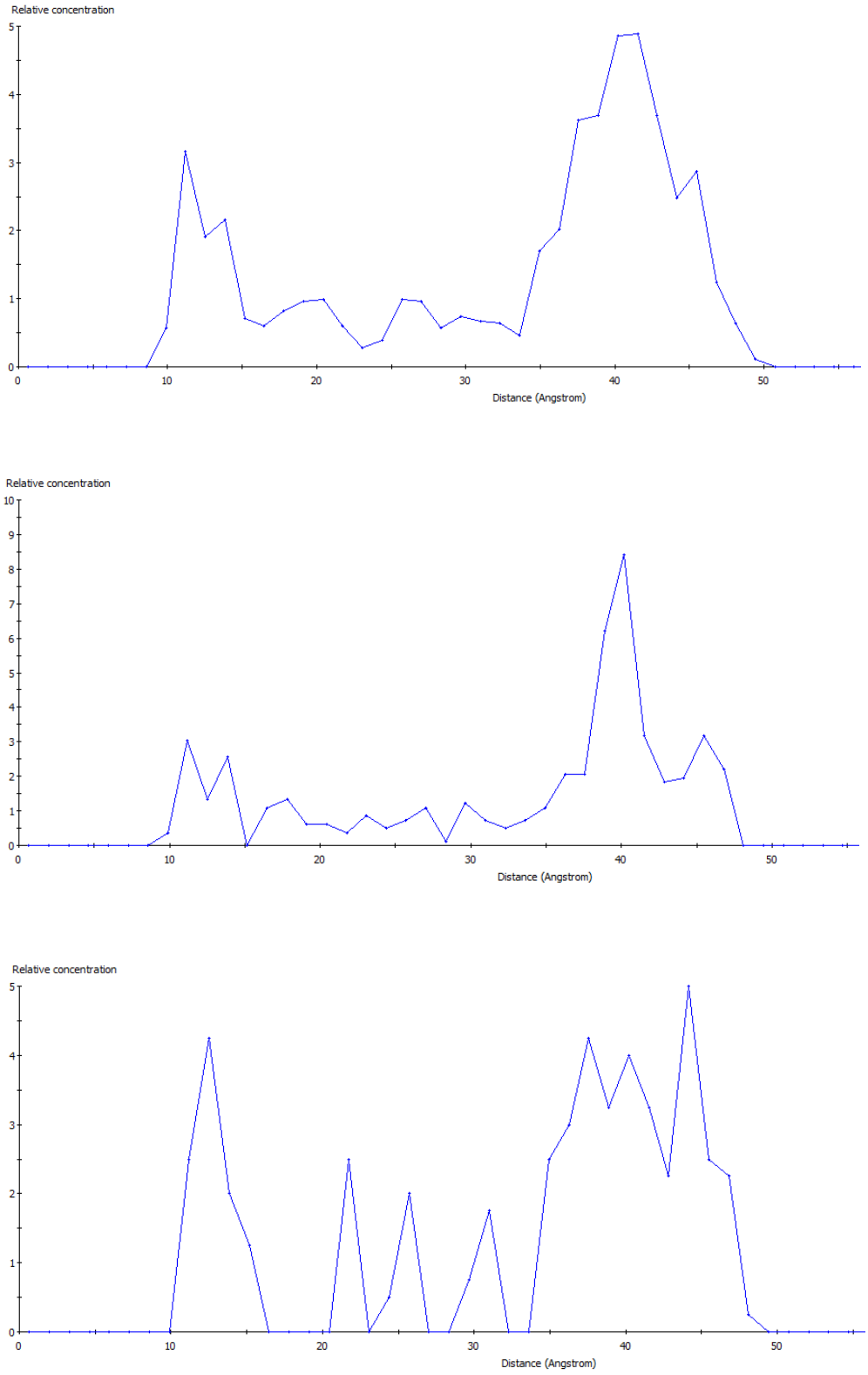

Figure 4-9 ***Concentration profiles of different atoms of groups on Ag (110)surface: (a) hydrogen, (b) oxygen and (c) nitrogen atoms after the MD calculation***

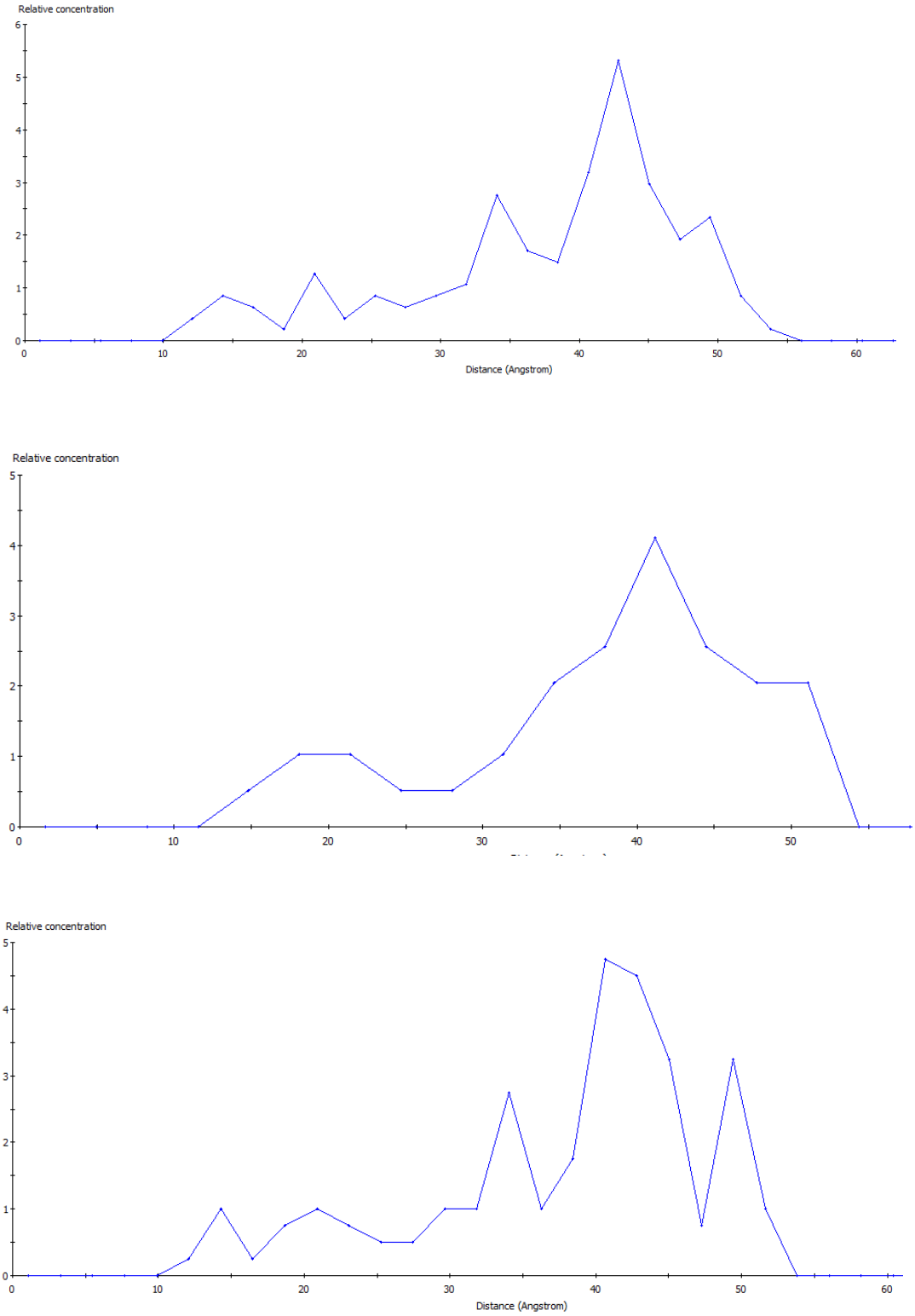

Figure 4-10 ***Concentration profiles of different atoms of chitosan backbone on Ag surface: (a) hydrogen, (b) oxygen and (c) carbon atoms before the MD calculation***

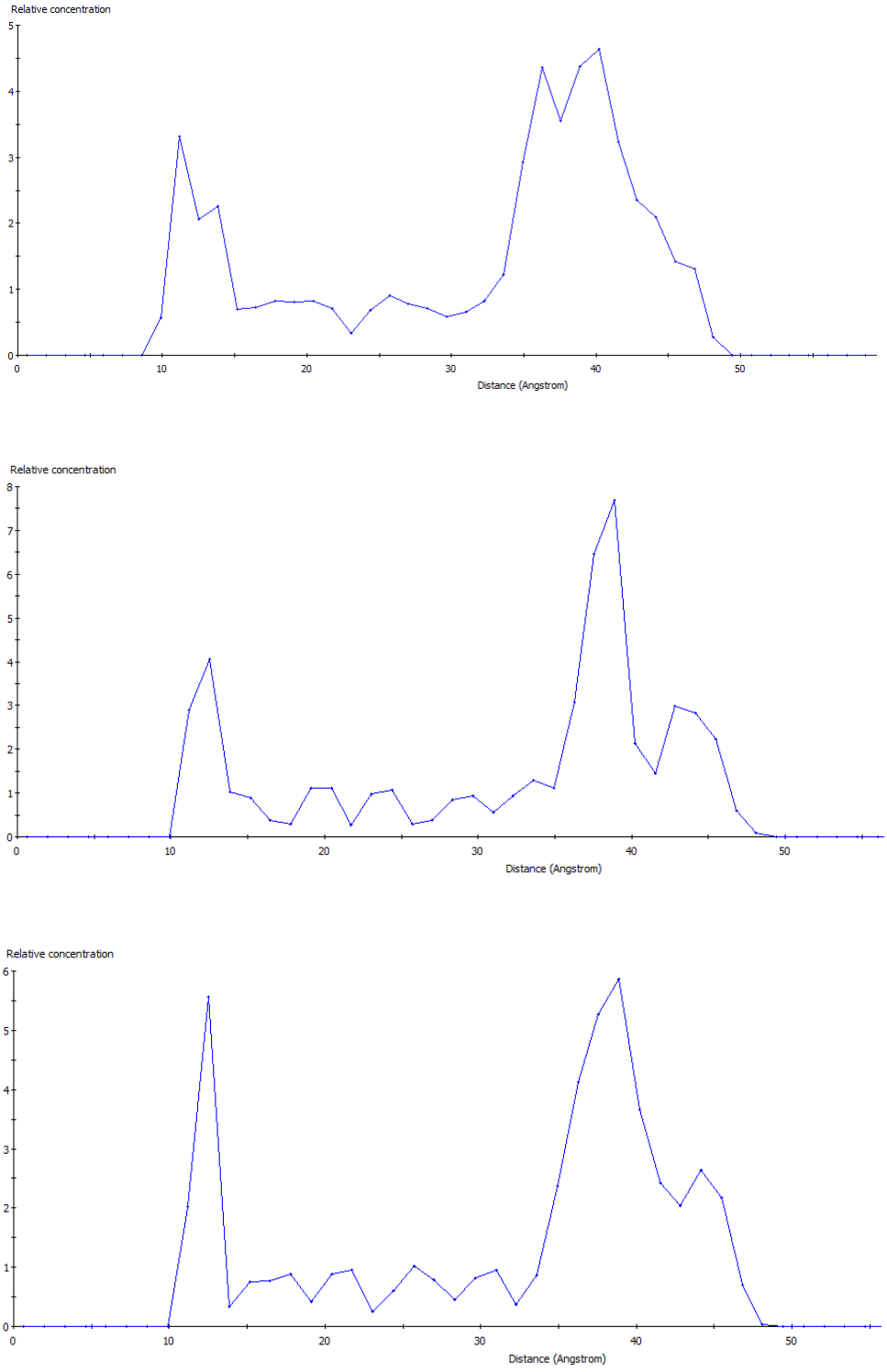

Figure 4-11 ***Concentration profiles of different atoms of chitosan backbone on Ag (111) surface: (a) hydrogen, (b) oxygen and (c) carbon atoms after the MD calculation***

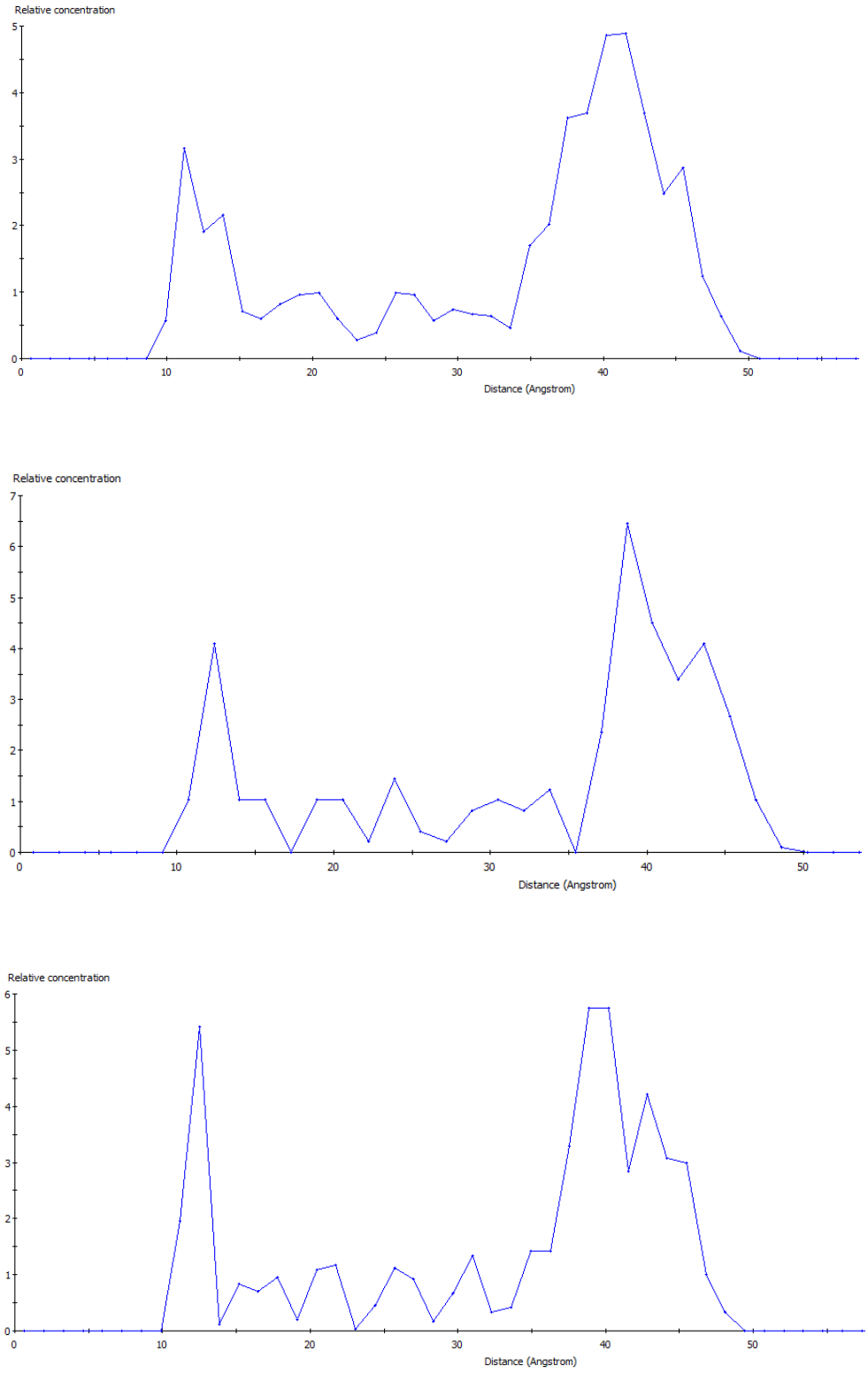

Figure 4-12 ***Concentration profiles of different atoms of chitosan backbone on Ag (110) surface: (a) hydrogen, (b) oxygen and (c) carbon atoms after the MD calculation***

4.4.4 Radial distribution function of atoms

The interaction between chitosan and Ag surface could be studied by the calculating the distance between the atoms of chitosan and the atoms of Ag surface on the atom scale.

The radial distribution function (RDF) represent the probability of density of A and B at a distance of r with respect to the bulk phase in a completely random distribution. RDF is defined as eq.

$$\mathbf{g_{AB}}(\boldsymbol{r}) = \frac{\boldsymbol{V}\langle\Sigma_{\boldsymbol{i}\neq\boldsymbol{j}}\boldsymbol{\delta}(\boldsymbol{r} - |\boldsymbol{r_{Ai}} - \boldsymbol{r_{Bj}}|)\rangle}{(\boldsymbol{N_A N_B} - \boldsymbol{N_{AB}})\boldsymbol{4\pi r^2 dr}} \quad (4\text{-}2)$$

where i and j refer to the ith and jth atoms of group A of N_A atoms and group B of N_B atoms, N_{AB} is the number of atoms common to both groups A and B, angle brackets imply averaging over different configurations [70].

As mentioned above, the atoms of groups were closer to the surface comparing to the atoms of chitosan backbone. The distance between the hydrogen atoms of groups and the surface were similar to the length of the hydrogen bond. Hydrogen bond is the interaction of a hydrogen atom with an electronegative atom, such as nitrogen, oxygen or fluorine that comes from another molecule or chemical group. There were many intramolecular hydrogen bonds in the chitosan chain, which cause the helical conformation. The distance of different atoms were calculated by the RDF of Forcite Module. The first peak position defines as the closest distance between two atoms, and the peak height represents the probability that the two atoms appear in this distance.

The RDF between hydrogen atoms which from hydrogen and amino groups of chitosan and silver atoms of surfaces as shown in Fig. 4-13(a) and Fig. 4-14(a). The first peak of (111) system is located at 1.2 Å and its height was higher than the (110) system. Therefore, the probability of formed hydrogen bonds between the hydrogen atoms and the silver atoms of (111) surface is higher. The reason might be that the silver atoms of (111) surface had the high activity, they could interact with other atoms easily.

Except hydrogen bonds, there might be another interaction between chitosan and surface of Ag. The interaction might be formed between the silver atoms and the oxygen or nitrogen atoms of

groups in chitosan. The RDF between oxygen atoms and silver atoms was shown in Fig. 4-13 (b) and Fig. 4-14 (b). The first peak of (111) surface was located in 2.7 Å and the one of (110) was in 2.8 Å. The radius of the oxygen atom and silver atom are 0.48 Å and 1.26 Å respectively. The sum of their radius was similar to the distance from each other. Thus, some interactions might be occurred between oxygen and silver atoms. Due to that the distance of two atoms, which (111) system is closer than (110) system, the probability of interaction between oxygen and silver atoms of (111) system is higher.

From the Fig. 4-13 (c) and Fig. 4-14 (c), the first peak which is belong to (111) system was located in 3.2 Å and the one which is belong to (110) system was in 2.9Å. The radius of the nitrogen is 0.75 Å. From the conclusion above, the probability of interaction between nitrogen and silver atoms of (110) system is higher than (111) system. The result was fit for the concentration profile of nitrogen atoms of the two systems. In my opinion, the most likely interaction was eq.

$$-NH_2 - e^- = -NH^{3+}; \quad Ag + e^- = Ag^0;$$

$$Ag^0 + Ag^0 = Ag_2{}^0; \quad Ag^0 + Ag = Ag_2{}^+;$$

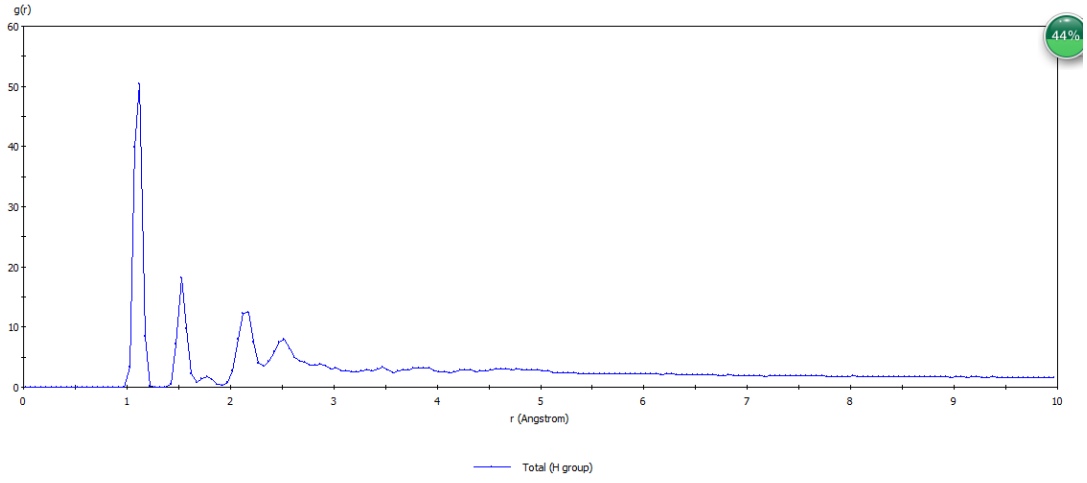

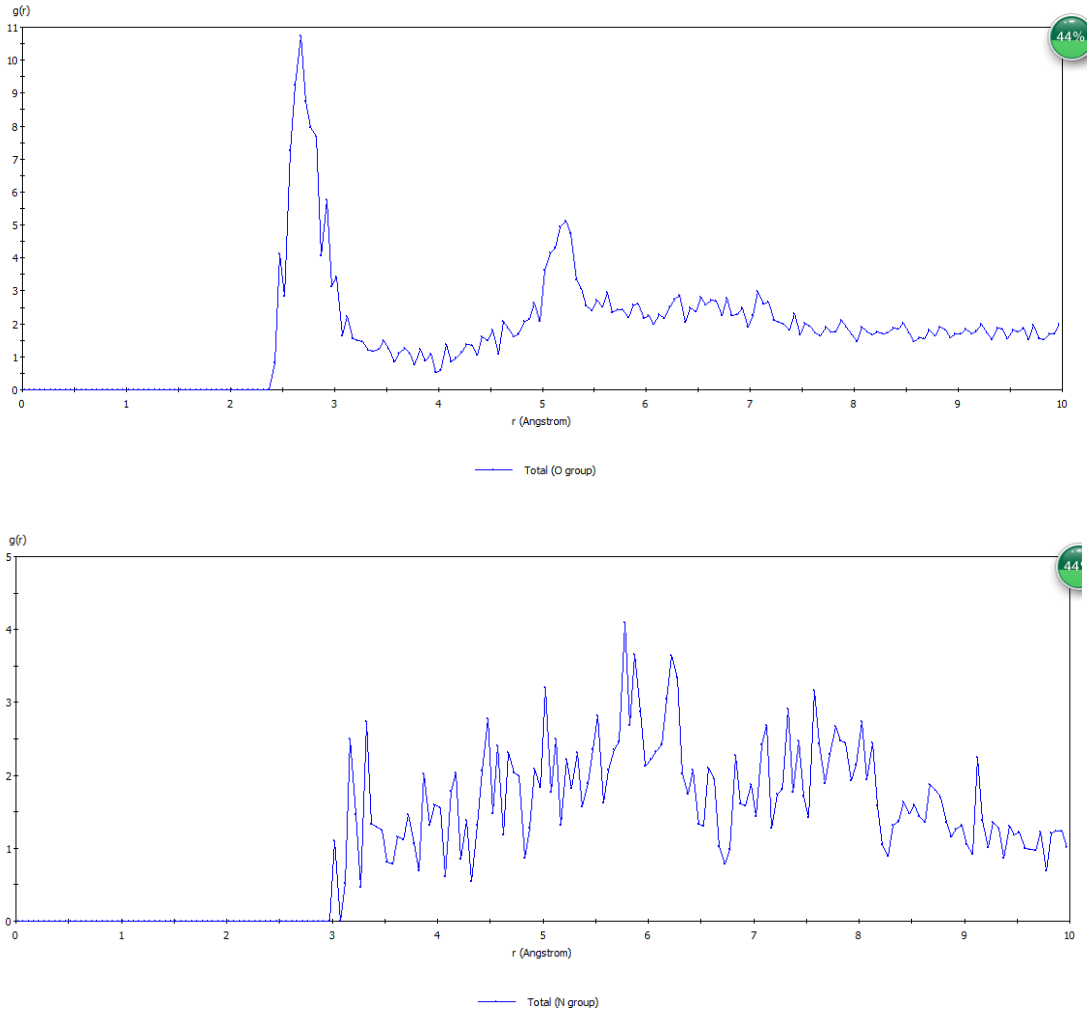

Figure 4-13 ***The radial distribution function between different atoms of the groups and the silver atoms from the (111) surface: (a) hydrogen, (b) oxygen and (c) nitrogen.***

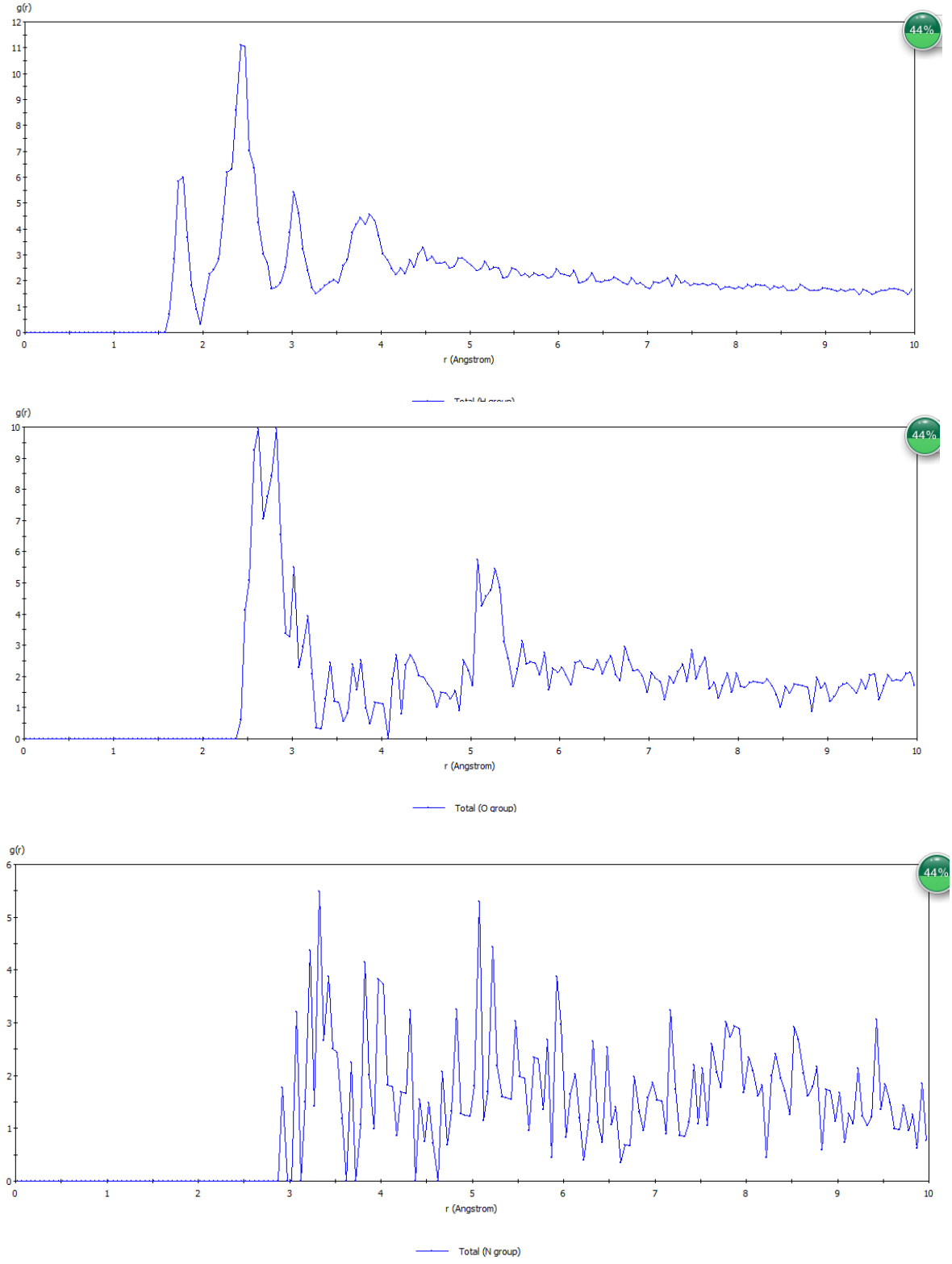

Figure 4-14 ***The radial distribution function between different atoms of the groups and the silver atoms from the (110) surface: (a) hydrogen, (b) oxygen and (c) nitrogen***

5. Atomic-scale interactions of the interface between chitosan and Pd

5.1 Pd model

In this study, the initial coordinates of Ag were taken from the crystallography open database. The (1 1 1), (1 1 0) and (0 0 1) surfaces of Ag were chosen to study the interaction with chitosan, because they were the dominant surfaces observed in experiments. The surfaces of Ag were built by cleaving the crystal along the crystallographic planes. The dimensions of the Pd surfaces were as follows: Pd (1 1 1), 19.25 Å×19.25 Å×6.74 Å (a×b×c), α = β = 90◦, γ = 120◦; Pd (1 1 0), 19.45 Å×19.25 Å×9.62 Å, α = β = γ = 90◦; Pd (0 0 1), 19.25 Å×19.25Å×13.61 Å, α = β = γ = 90◦; (see Fig. 5-1). The minimization process was completed by the steepest descent method with the convergence of 1000kcal/mol and the conjugate gradient method with the convergence of 10 kcal/mol.

5.2 Interface model

The optimized chitosan chain was added onto the built Pd surfaces, and then the "vacuum slab" with the height of 10Å was put upon the chitosan– Pd system with 3D periodic boundary conditions. The initialization model of the Pd surface with the chitosan was shown in Fig. 5-2. The surfaces of Pd were fixed before simulations. The MD simulations of the adsorption of chitosan on Pd surface were studied in the canonical ensemble (NVT) at 298 K. The temperature of the systems was kept through the Andersen method. The time step was 1.0 fs and the dynamics balance time was 200.0 ps. And the whole MD simulation was performed under the same conditions to record the trajectory of all the atoms in the system. After reaching equilibrium state, the binding energy between the chitosan chain and the Pd surfaces were calculated to evaluate the interfacial interactions. The concentration profiles of the atoms (in the oxygen and amino groups of the chitosan) and the atoms (in the chitosan backbone) were used to examine the activity of groups and backbone of the chitosan during the adsorption process. The

radial distribution function (RDF) of different atoms could be used to understand the interaction of chitosan/ Pd on the atom scale.

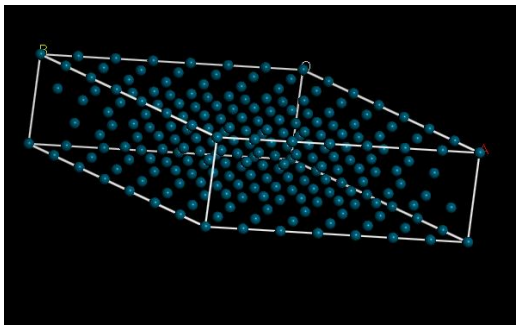

Figure a

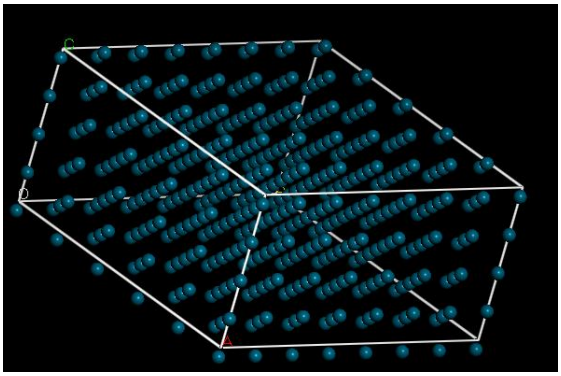

Figure b

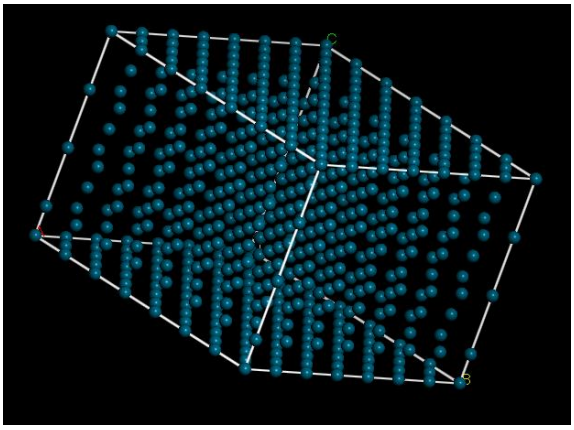

Figure c

Figure 5-1 the model of the Pd (1 1 1), (1 1 0) and (0 0 1) surfaces as Figure a, b, and c

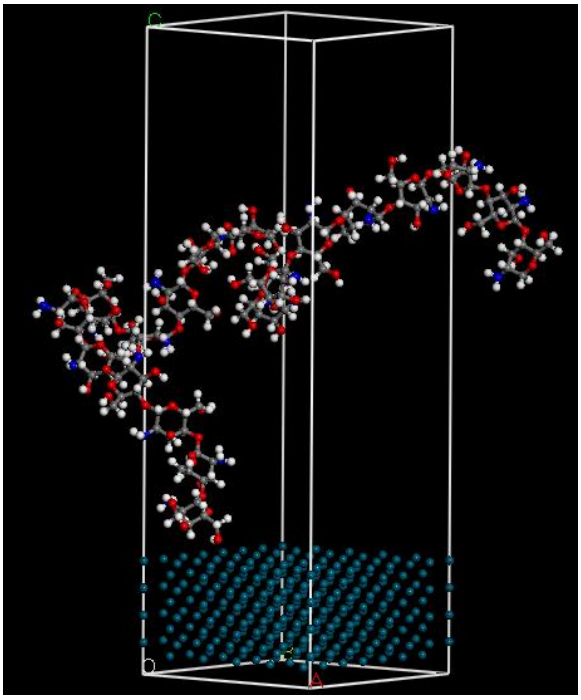

Figure 5-2 the interface between chitosan and Ag surface

5.3 Certification of the balance of the system

When study the properties of the system, the balance of the system is the fundamental problem to make sure. All the factors as temperature, density, energy are able to help to judgment the balance of the system.

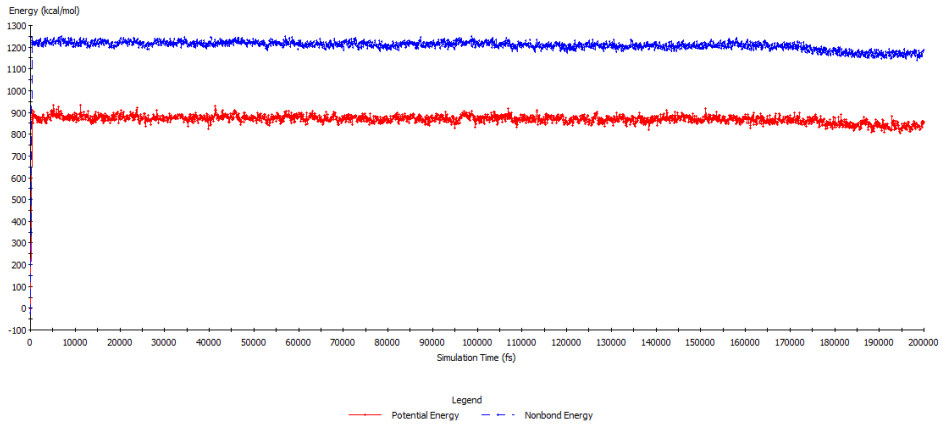

Figure 5-3 Energy fluctuation properties of Chitosan

In this work, the most usual method is used to test the balance which is using the temperature and energy. When the system energy was stable at the certain range and the temperature was

change slightly during the set value, the system approached to balance condition. The curve of the energy change and the temperature change were shown in the Fig.5-3 and Fig.5-4.

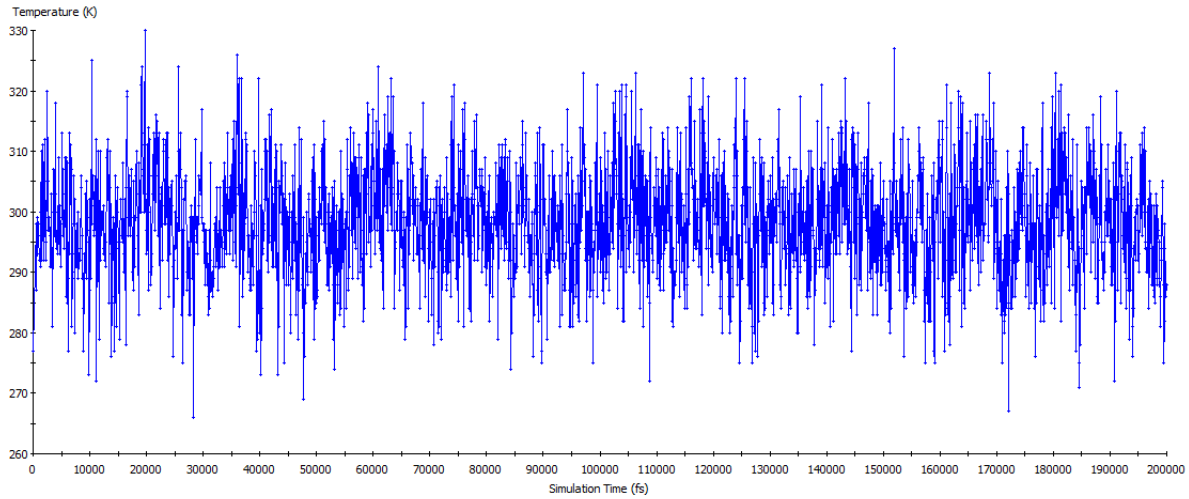

Figure 5-4 ***Temperature fluctuation properties of Chitosan***

5.4 Result and discussion

5.4.1 The interaction energy between chitosan and Pd

Table 5-1 presented the interaction energy of chitosan/Pd. It can be found that the value of E_i between chitosan and (1 1 0) surface was larger than that of the other surface. Therefore, the interaction between chitosan and (1 1 0) surface was greater than those of (1 1 1) and (0 0 1) surfaces, the interface interactions between chitosan/ (1 1 0) surface and chitosan/ (0 0 1) surface were very similar. Moreover, the surface free energy was nearly equal between (1 1 0) and (0 0 1) surfaces and they had similar surface structures. Therefore, we choose (1 1 1) and (0 0 1) surfaces for the following study.

Table 5-1 the interaction energy between different Pd surfaces and Chitosan

Pdsurface	Area(Å^2)	E_{total}(kcal mol^{-1})	$E_{polymer}$(kcalmol^{-1})	E_{Pd}(kcal mol^{-1})	E_i(kcal mol^{-1})
(1 1 1)	370.56	4404.38	1077.23	5210.60	5.083
(1 1 0)	37056	16953.41	1073.49	17877.51	6.36
(0 0 1)	374.41	10019.55	1080.14	10975.48	5.438

5.4.2 The chain behavior of chitosan on Pd surface

Between chitosan and inorganic surface, there might be some physical and chemical interactions after adsorption. These interactions might lead to the configuration changes of chitosan and the changes of molecular models were able to observe by Molecular Dynamics simulation on both before and after adsorption. In this work, all the chitosan of different interfaces had the same initial configuration (see Fig.5-5(a)).

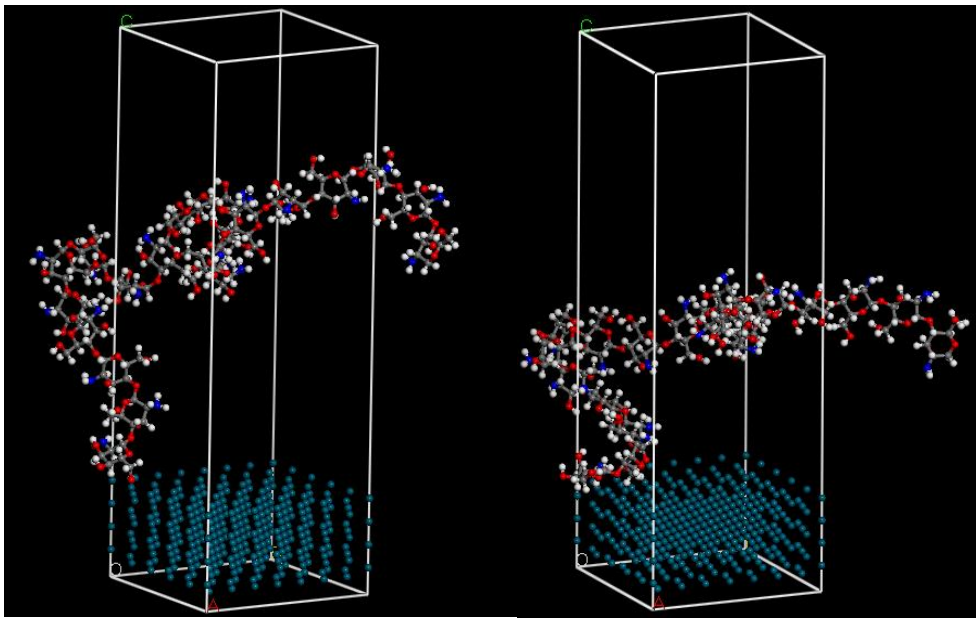

Figure a *Figure b*

Figure 5-5 the configuration of chitosan chain on Pd (1 1 0) surface (a) before MD simulation (b) after MD simulation

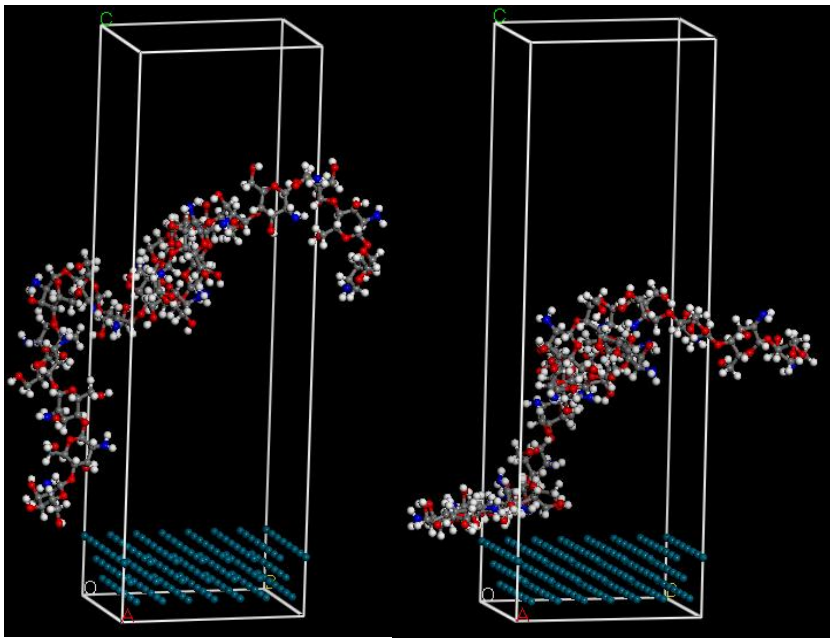

Figure a *Figure b*

Figure 5-6 The configuration of chitosan chain on Pd (1 1 1) surface (a) before MD simulation (b) after MD simulation

The structures of the chitosan on (1 1 0) and (1 1 1) surfaces after MD simulation were shown in the Fig.5-5 and Fig.5-6. It could be seen that chitosan chain before simulation was the helical conformation and loosely stretched. And the hydrogen and amino groups in both sides of the chitosan chain. After MD simulation, the chain was trend to move to the Pdsurface. The stretched chain was trend to huddle up.

5.4.3 The concentration profile

The concentration profile was a function of the positions along the axes of the Pd surface and a distribution of the specific atom or group in the polymer. In this work, the concentration profile of hydrogen, oxygen, nitrogen atoms on the chitosan was choose along the axis normal to Pd surface. Firstly, the concentration profile if hydrogen atoms from the hydrogen and amino groups on the chitosan chain on the different surfaces. Before the MD simulation, the concentration profile was located in the range of 35-50 Å as shown in Fig.5-7. However, after the MD simulation, the other peak of the concentration profiles of hydrogen atoms on (1 1 1) surface and (0 0 1) were observed in the range of 10-12 Å. This was a very close distance between hydrogen atoms and Ag surfaces which might lead to the interaction. The strongest interaction was occurred in the closest distance which is the location of first peak. And the normalized are was used to compare the concentration distribution of the atom which have the closer distance on the surface. From the Fig.5-8(a) and Fig.5-9(a), the first peak of chitosan/ (1 1 1) surface was located in 12 Å; and the first peak of chitosan/ (1 1 0) surface was also located in 12 Å. Then, the normalized area of (1 1 1) which was obviously bigger than that of (1 1 0).This means there were more hydrogen atoms on the (1 1 1) surface in the closest distance than on the (1 1 0) surface. Therefore, there might be stronger interaction of hydrogen atoms/ (1 1 1) surface than hydrogen atoms/ (1 1 0) surface.

The concentration of oxygen atoms that belong to the hydrogen group of chitosan on the different surfaces were studied as shown inFig.5-8(b) and Fig.5-9(b). Before the MD simulation, the concentration profile was located in the range of 30-50 Å as shown in Fig.5-7. However, from the concentration profiles of hydrogen atoms on (1 1 1) surface and (1 1 0) after the MD simulation, the first peak of profiles were located in 11 Å. And the normalized area of (1 1 1)

which was also bigger compare to the area of (1 1 0).Therefore, there were more oxygen atoms of hydrogen groups on the (1 1 1) surface in the closest distance.

Fig.5-8(c) and Fig.5-9(c) showed the concentration profiles of nitrogen atoms on chitosan/ (1 1 1) surface and chitosan/ (1 1 0) surface. And the normalized area of the first peak of (1 1 0) which was also bigger compare to the area of (1 1 1). Therefore, there were more oxygen atoms of hydrogen groups on the (1 1 0) surface in the closest distance.

The concentration profiles of carbon, oxygen and hydrogen atoms from the chitosan backbone on the different surfaces were shown in Fig.5-10, Fig. 5-11and Fig.5-12. Compared with the atoms of hydrogen and amino groups on the chitosan chain, the atoms from backbone had a longer distance from the Pd surface. It means that the interaction between chitosan Pdmight mainly come from the groups of chitosan.

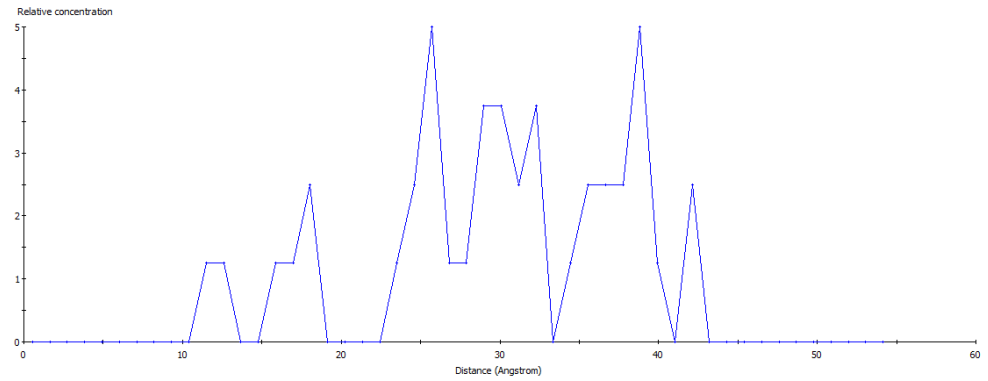

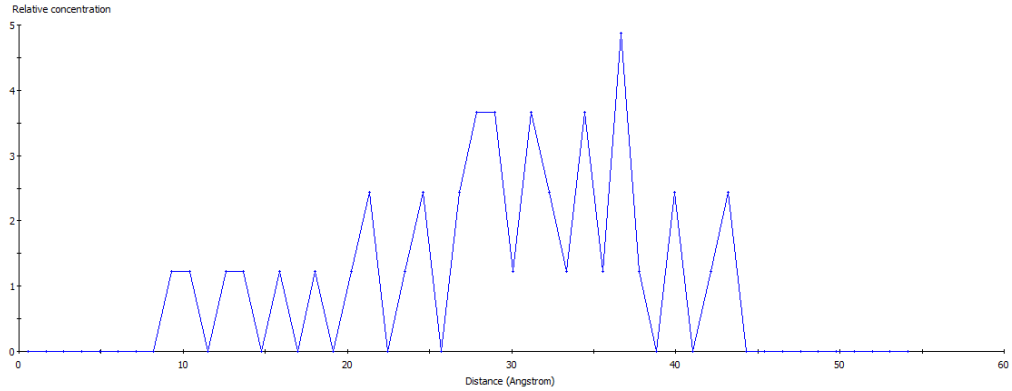

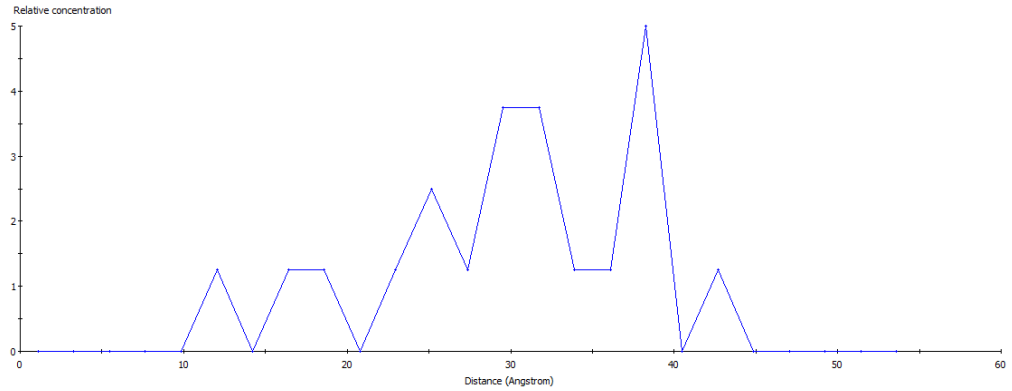

Figure 5-7 ***Concentration profiles of different atoms of groups on Pd surface: (a) hydrogen, (b) oxygen and (c) nitrogen atoms before the MD calculation***

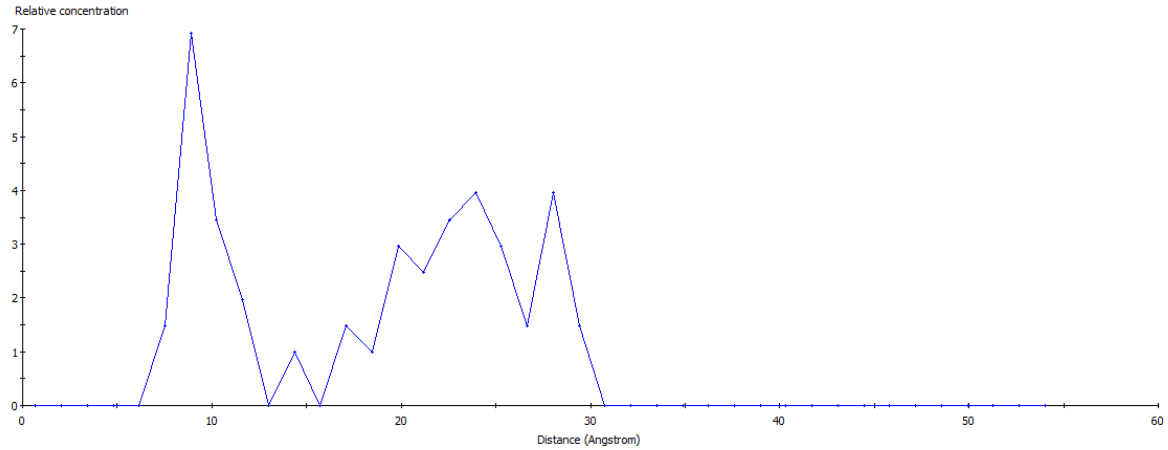

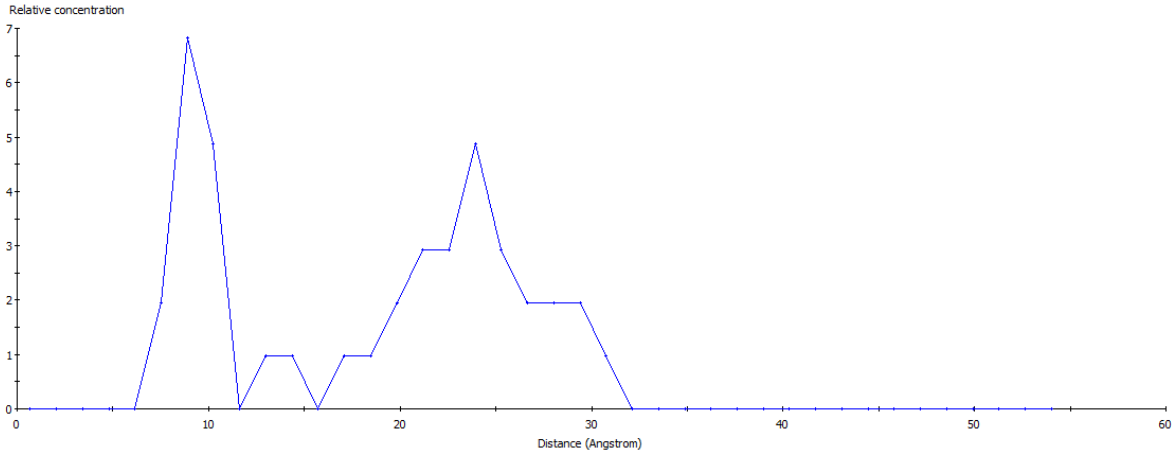

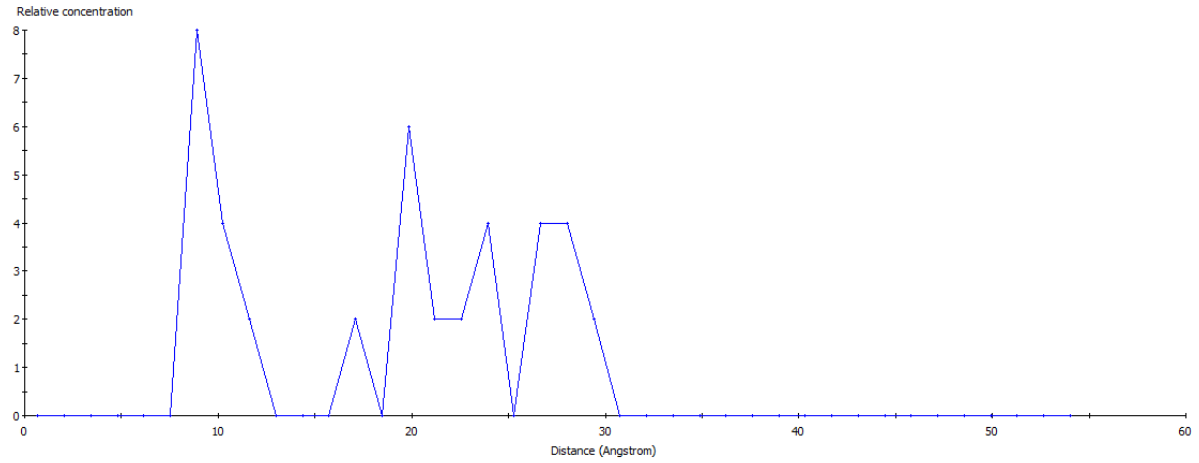

Figure 5-8 ***Concentration profiles of different atoms of groups on Pd (111) surface: (a) hydrogen, (b) oxygen and (c) nitrogen atoms after the MD calculation***

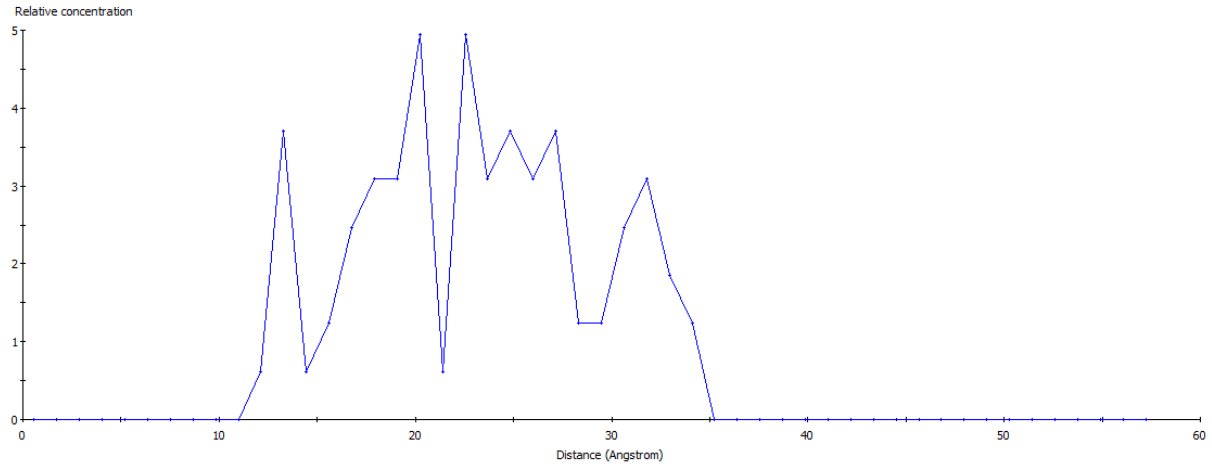

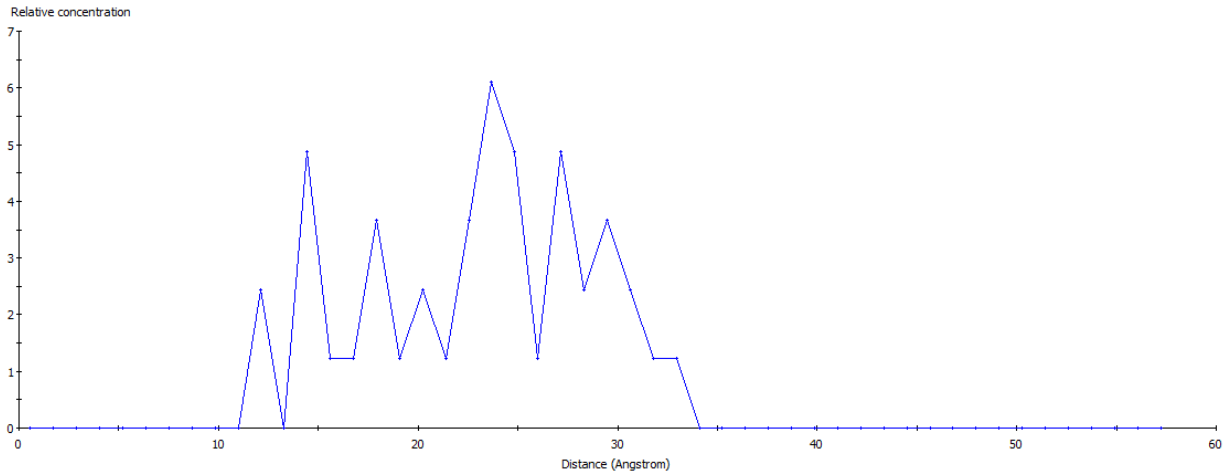

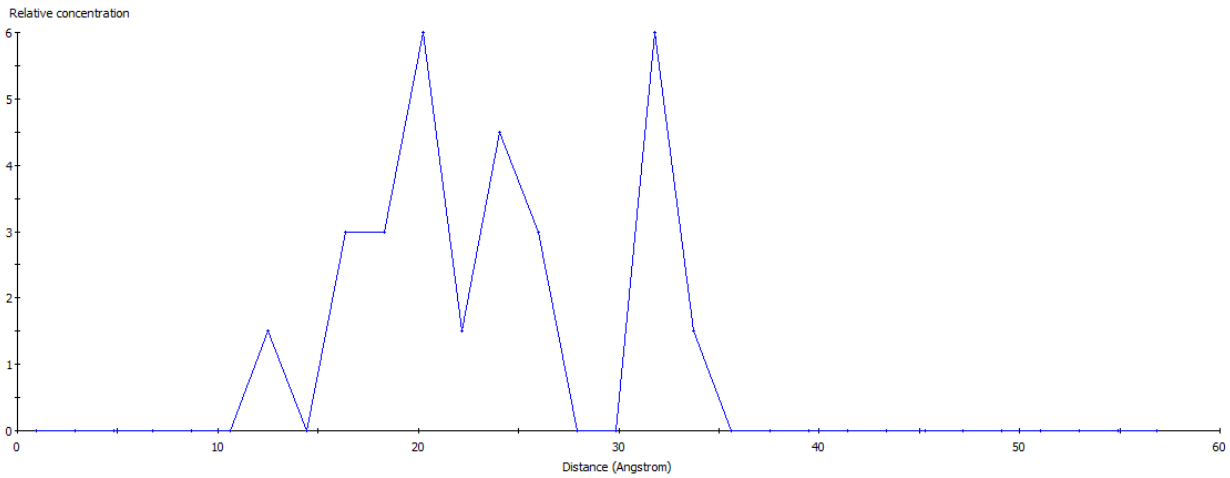

Figure 5-9 ***Concentration profiles of different atoms of groups on Pd (110) surface: (a) hydrogen, (b) oxygen and (c) nitrogen atoms after the MD calculation***

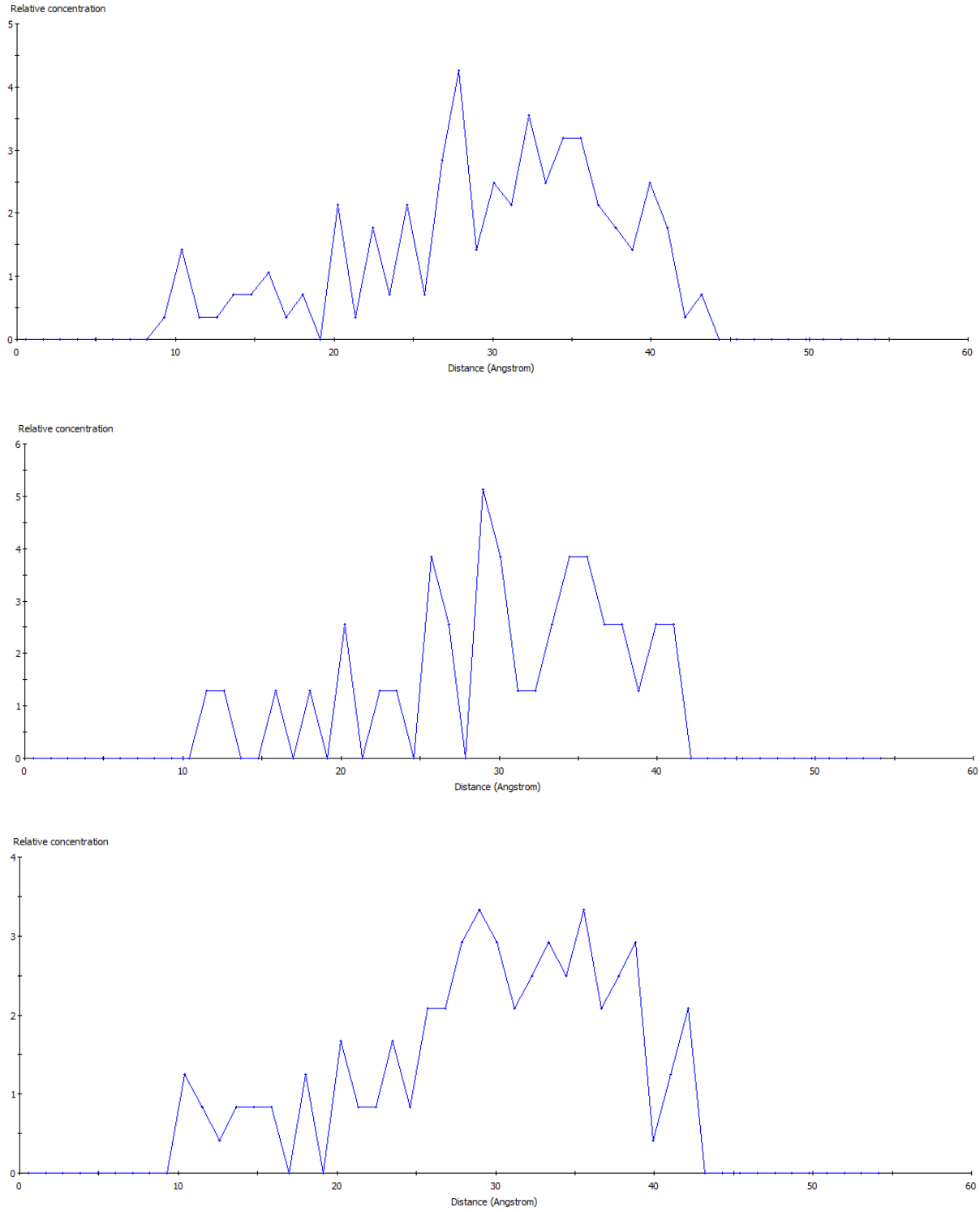

Figure 5-10 ***Concentration profiles of different atoms of chitosan backbone on Pd surface: (a) hydrogen, (b) oxygen and (c) carbon atoms before the MD calculation***

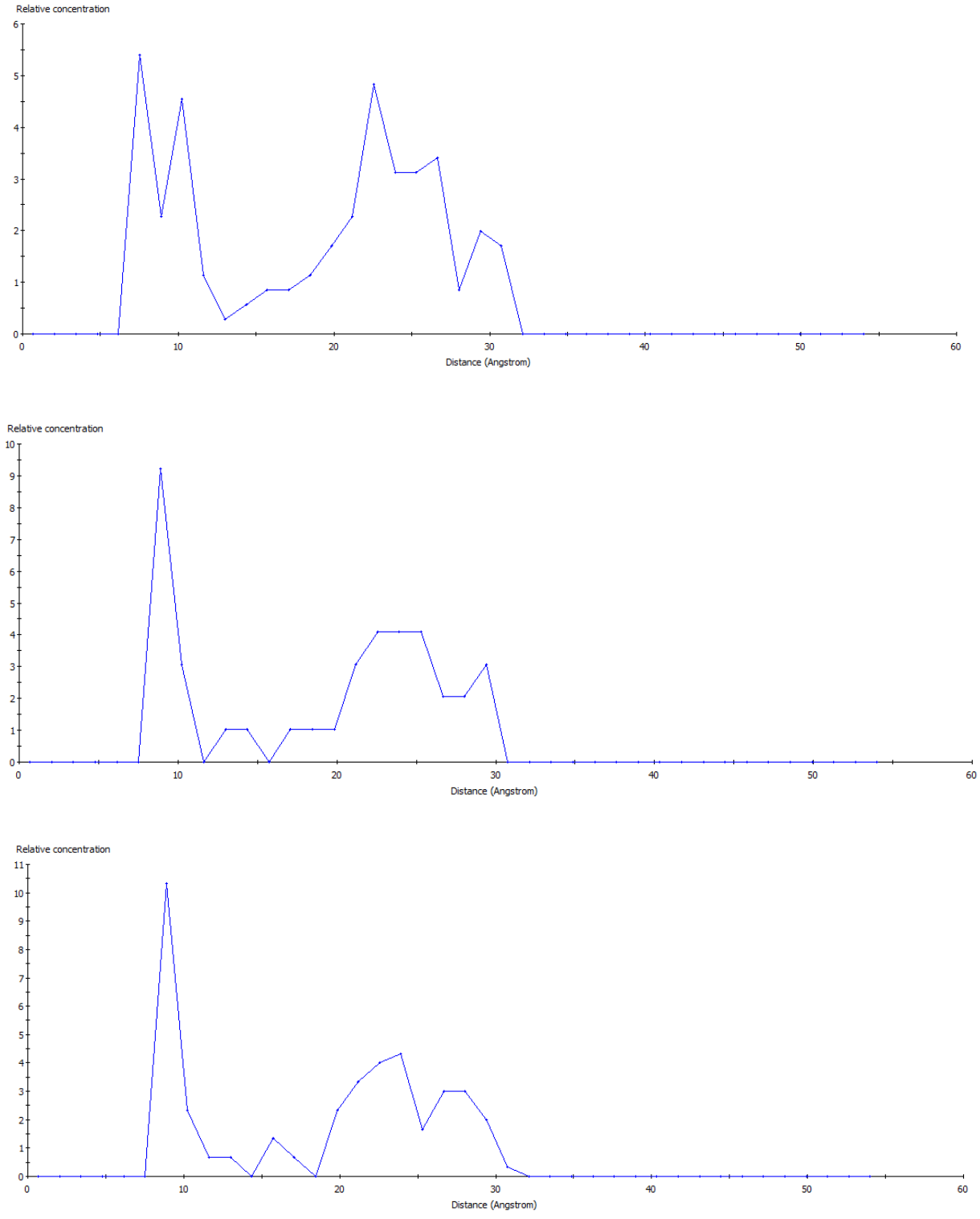

Figure 5-11 ***Concentration profiles of different atoms of chitosan backbone on Pd (111) surface: (a) hydrogen, (b) oxygen and (c) carbon atoms after the MD calculation***

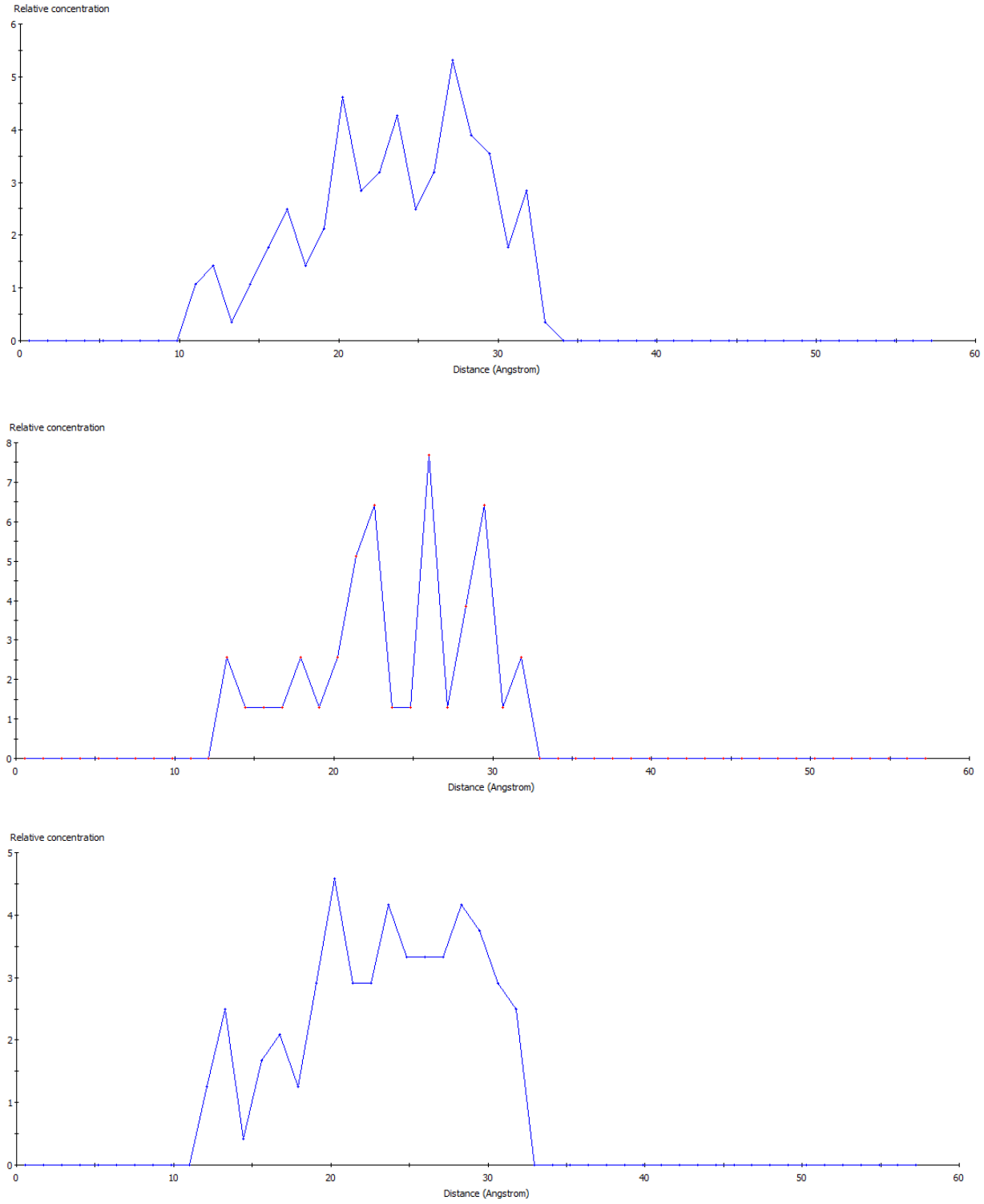

Figure 5-12 ***Concentration profiles of different atoms of chitosan backbone on Pd (110) surface: (a) hydrogen, (b) oxygen and (c) carbon atoms after the MD calculation***

5.4.4 Radial distribution function of atoms

The distances between the atoms of chitosan and Pd surface were studied by the RDF.

The RDF between hydrogen atoms which from hydrogen and amino groups of chitosan and palladium atoms of surfaces as shown in Fig. 5-13(a) and Fig. 5-14(a). The first peak of (111) system is located at 1.6 Å and its height was higher than the (110) system. Therefore, the probability of formed hydrogen bonds between the hydrogen atoms and the palladium atoms of (111) surface is higher. The reason might be that the palladium atoms of (111) surface had the high activity, they could interact with other atoms easily.

Except hydrogen bonds, there might be another interaction between chitosan and surface of Pd. The interaction might be formed between the palladium atoms and the oxygen or nitrogen atoms of groups in chitosan. The RDF between oxygen atoms and palladium atoms was shown in Fig. 5-13 (b) and Fig. 5-14 (b). The first peak of (111) surface and (110) surface was both located in 2.6 Å. The radius of the oxygen atom and palladium atom are 0.48 Å and 0.86 Å respectively. Compare to the distance from each other, the sum of their radius was far away. Thus, the interactions occurred between oxygen and palladium atoms were relatively weak.

From the Fig. 5-13 (c) and Fig. 5-14 (c), the first peak which is belong to (111) system was located in 2.8 Å and the one which is belong to (001) system was in 3.2 Å. The radius of the nitrogen is 0.75 Å. From the conclusion above, the probability of interaction between nitrogen and palladium atoms of (111) system is higher than (110) system. The result was fit for the concentration profile of nitrogen atoms of the two systems. In my opinion, the most likely interaction was shown as blow:

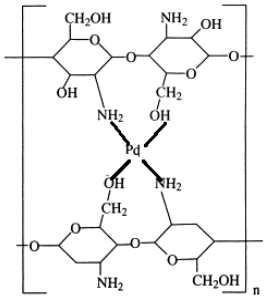

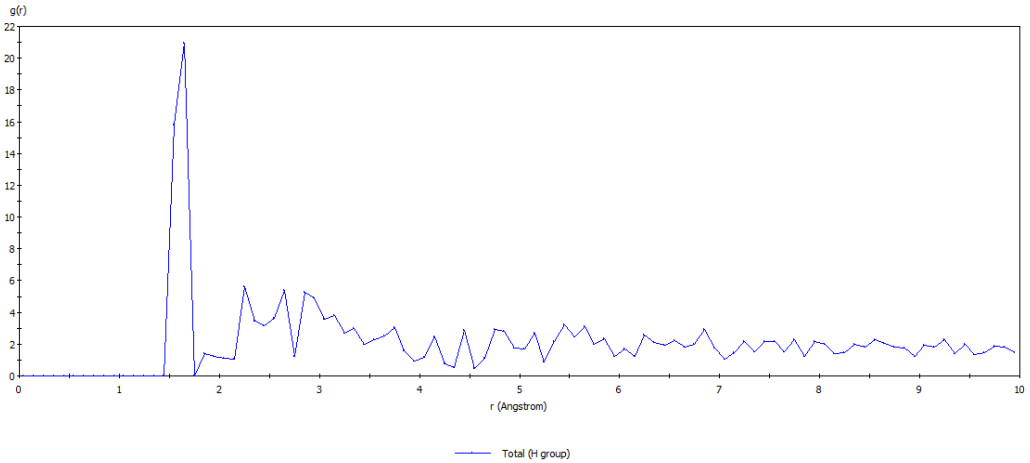

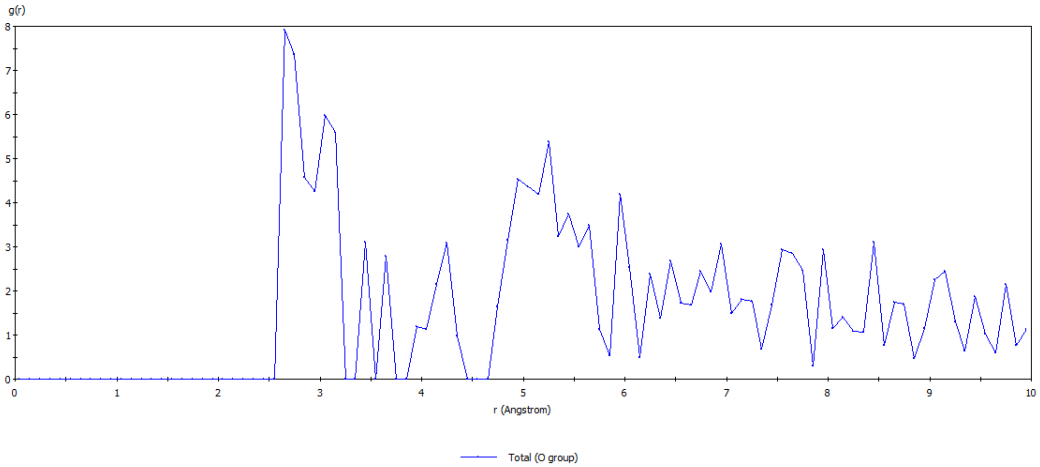

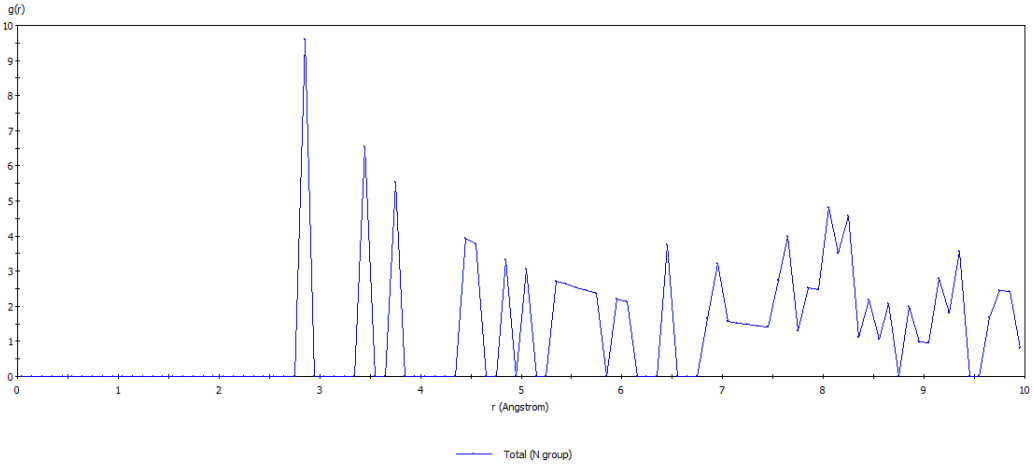

Figure 5-13 the radial distribution function between different atoms of the groups and the palladium atoms from the (111) surface: (a) hydrogen, (b) oxygen and (c) nitrogen.

Fig.5-14 The radial distribution function between different atoms of the groups and the palladium atoms Figure 5-14from the (110) surface: (a) hydrogen, (b) oxygen and (c) nitrogen.

6. Conclusion

1. Due to the calculated result of the solubility parameter δ , the length of chitosan was chosen 20 repeated units.

2. Through Mechanical Modeling of chitosan chain, the simulation result of the glass transition temperature of chitosan was similar to the experiment value as 476K.

3. The water content of chitosan was able to effect the glass transition temperature obviously.

4. The interaction energy between chitosan and different metal surfaces indicates that the interaction of chitosan and silver (1 1 0) surfaces is stronger than that of (1 1 1) and (0 0 1) surface.

5. The interaction of chitosan and palladium (1 1 0) surfaces is stronger than that of (1 1 1) and (0 0 1) surface.

6. The concentration profiles show that hydrogen and amino groups of chitosan could form strong interactions with the surfaces of metal. The radial distribution function show that the probability of forming the nitrogen atoms and metal on the surface have physical interactions.

References:

[1]Barbier D, Brown D, Grillet A, et al. Interface between end-functionalized PEO oligomers and silica nanoparticle studied by molecular dynamics simulations [J]. Macromolecules, 2004 37:4695 4710

[2] Moore T T, Koros W J. Non-ideal effects in organic-inorganic materials for gas separation membranes [J] Mole Sturct, 2005, 739: 87-98

[3] M.F.A. Goosen (Ed.), Applications of Chitin and Chitosan, Technomic, Lancaster, 1997.

[4] Kim HW, Knowles JC, Salih V, Kim HE. Hydroxyapatite and fluorhydroxyapatite layered film on titanium processed by sol–gel route for hardtissue Implants. J Biomed Mater Res 2004; 71B:66–76.

[5] Gomez-Vega JM, Saiz E, Tomsia AP, Marshall GW, Marshall SJ. Bioactive glass coatings with hydroxyapatite and bioglass particles on Ti-based implants. 1. Processing. Biomaterials 2000; 21:105–11.

[6] Limm W, Hollifield H C. Effects of temperature and mixing on polymer adjuvant migration to corn oil and water [J]. Food Additives and Contaminants, 1995, 14 (4): 609 一 624

[7] Baner A, Brandsch J, Franz R, et al. The application of a predictive migration model for evaluating the compliance Additives and Contaminants of plastic materials with European food regulations [J]. Food 1996, 13(5): 587 一 601

[8] Limm W, Hollifield H C. Modeling of additive diffusion in polyolefins [J]. Food Additives and Contaminants, 1996, 13(8): 949-967

[9] Lickly T D,Rainey M. L, Burgert L C, et al. Using a Simple Diffusion Model to predict residual monomer migration considerations and limitations [J]. Food Additives and contaminants, 1997, (14): 65-74

[10] Brandsch J, Mercea P, et al. Migration modeling as a tool for quality assurance of food packaging [J]. Food Additives and Contaminants, 2002, 19: 29-41

[11]Begler T H. Methods and approaches used by FDA to evaluate the safety of food packaging materials [J]. Food Additives and Contaminants, 1997, 14(6-7): 545-553

[12] Obrien A, Cooper I. Polymer additive migration to foods 一 a direct comparison of experimental data and values calculated from migration models for polypropylene [J]. Food Additives and Contaminants, 2001, 18(4): 343 一 3_5_5

[13] 朱宇，陆小华，丁皓等.分子模拟在化工应用中的若干问题及思考 [fJl.化工学报，2004, 55(8): 1231 一 1223

[14] Zhu Y, Lu X H, Zhou J, et al. Prediction of diffusion coefficient for gas, liquid and supercritical fluid: application to pure real fluids and infinite dilute binary solutions based on the simulation of Lennard-Jones fluid [J]. Fluid Phase Equilib, 2002, 194-197: 114-11 _59

[15] Zhou J, Lu X H, Wang Y R, et al. Molecular dynamics investigation on the infinite dilute diffusion coefficients of organic compounds in supercritical carbon dioxide [J]. Fluid Phase Equilib, 2000, 172(2): 279-291

[16] F.M. Al Kharafi, A.M. Abdullah, I.M. Ghayad, B.G. Ateya, Appl. Surf. Sci. 253 (2007) 8986.

[17] Zhou J, Wang W C. Molecular simulation [J]. Chinese Jour of Chem Eng, 2001 9(1): carbon dioxide adsorbed in a sfit carbon

[18] Zhou J, Wang W C. Adsorption and diffusion [J]. Langmuir, 2000, 16(21):8063 一 8070-38 of supercritical carbon dioxide in slit pore

[19] Molecular dynamics simulation on diffusion properties of chitosan and chitosan composite membranes TB324-12596 2012

[20] Sun H. Ab initio calculations and force field development for computer simulation of polysilanes [J]. Macromolecules, 1995, 28: 701-712

[21]Sun H. COMPASS: an ab initio force-field optimized for condensed-phase application overview with details on alkane and benzene compounds [J]. J Phys Chem B, 1998, 102:7338-7364

[22] Metropolis N, Rosenbluth A W, Rosenbluth M N. Equation of state calculations by fast computing machines [J]. J Chem Phys, 1953, 21(6): 1087 — 1093

[23] Beman D. Some mutistep method for use in molecular dynamics calculations [J]. Journal of Computer Physics, 1976, 20(2): 130 — 138

[24] Verlet L. Computer "experiment" on classical fluids. Thermodynamic properties of

Lennard-Jones molecules [J]. Physical Review, 1967, 159(1): 98-103

[25] Swope W C, Anderson H C, Berens P H. A computer simulation method for the calculation Application of equilibrium constants for the formation of Physical clusters of molecules: to small water clusters [J]. J Chem Phys, 1982, 76(1):637 — 64_5

[26] Rahman A. Correlations in the motion of atoms in liquids argon [J]. Phys Rev a, 1964 136(2A): 405-413

[27] Honeycutt R W. The potential calculation and some applications method [J]. Journal of Computer Physics, 1970, 9(1): 136-211

[28] Koros W J. Barrer polymers andstructures [M]. Washington: ACS Symp. Ser 423, Am Chem, 1990

[29] Stern S A. Polymers for gas separation: the next decade [J]. J Membr Sci, 1994, 94(1):1 — 6_5

[30] Vieth W R, Howell J H, Hsieh J H. Dual sorption theory [J]. J Membr Sci, 1976, 1:177-220

[31]Stannett V T, Koros W J, Paul D R. Recent advances in membrane science and technology [J]. Adv Polym Sci, 1979, 32:69 — 121

[32] Frisch H L, Stern S A. Diffusion of small molecules in polymers [J]. Crit Rev Solid State Mater Sci, 1983, 11:123 — 187

[33] Van Gunsteren W F, Weiner P K. Computer simulation of biomolecular systems: theoretical and experimental applications [M]. Vol 2, Leiden:ESCOM, 1989,p11

[34] Baranyai A. Calculation of transport properties from molecular dynamics simulation [J].,J Phys Chem, 1994, 101(4):5070-5075

[35] Charati S. G., Stern S. A, Diffusion of gases in silicone polymer: molecular dynamics simulations [J]. Macromol, 1998, 31:5529-5535.

[36] Takeuchi H, Roe R J, Mark J. Molecular dynamics simulation of simple gas molecules in polymers (II): Effect of free volume distribution [J]. Journal of Chemical Physics, 1990, 93:9042-9048

[37] M Lundin, L Macakova, A Dedinaite, et al, Interactions between chitosan and SDS at a low-charged silica substrate compared to interactions in the bulk-the effect of ionic strength [J]. Langmuir, 2008, 24: 3814-3827

[38] S. R.White, N. R. Sottos, P. H. Geubelle, J. S. Moore, M. R. Kessler,S. R. Sriram, E. N. Brown and S. Viswanathan, Nature, 2001, 409,794.

[39] E. N. Brown, S. R. White and N. R. Sottos, Compos. Sci. Technol., 2005, 65, 2474.

[40] D. G. Shchukin, M. Zheludkevich, K. A. Yasakau, S. Lamaka,M. G. S. Ferreira and H. M€owhald, Adv. Mater., 2006, 18, 1672.

[41] M. L. Zheludkevich, S. K. Poznyak, L. M. Rodrigues, D. Raps,T. Hack, L. F. Dick, T. Nunes and M. G. S. Ferreira, Corros. Sci., 2010, 52, 602.

[42] R. Tomaszek, L. Pawlowski, L. Gengembre, J. Laureyns,Z. Znamirowski and J. Zdanowski, Surf. Coat. Technol., 2006, 201, 45.

[43] P. Shi, W. F. Ng, M. H. Wong and F. T. Cheng, J. AlloysCompd., 2009, 469, 286.

[44] A. Cha′vez-Valdez, M. Herrmann and A. R. Boccaccini, J.Colloid Interface Sci., 2012, 375, 102.

[45] Y. Sun and I. Zhitomirsky, Mater. Lett. , 2012, 73, 190.

[46] I. Corni, M. P. Ryan and A. R. Boccaccini, J. Eur. Ceram.Soc., 2008, 28, 1353.

[47] K. Kanamura and J. Hamagami, Solid State Ionics, 2004,172, 303.

[48] L. Besra and M. Liu, Prog. Mater. Sci., 2007, 52, 1.

[49] A. R. Boccaccini and I. Zhitomirsky, Curr. Opin. Solid StateMater. Sci., 2002, 6, 251.

[50] T. Moskalewicz, A. Czyrska-Filemonowicz and A.R. Boccaccini, Surf. Coat. Technol., 2007, 201, 7467.

[51] C. K. Lin, T. J. Yang, Y. C. Feng, T. T. Tsung and C. Y. Su, Surf. Coat. Technol., 2006, 200, 3184

[52] Long-Hao Li, Young-Min Kong, Hae-Won Kim, et al. Improved biological performance of Ti implants due to surface modification by micro-arc oxidation. Biomaterials, 2004, 25: 2867～2875

[53] Yaming Wang, Bailing Jiang, Tingquan Lei,et al. Dependence of growth features of microarc oxidation coatings of titanium alloy on control modes of alternate pulse. Materials Letters, 2004, 58: 1907～1911

[54] Wenbin Xue, Chao Wang, Ruyi Chen. Structure and properties characterization of ceramic coatings produced on Ti-6Al-4V alloy by microarc oxidation in aluminate solution. Materials Letters, 2002, 52:435～441

[55] Yaming Wang, Tingquan Lei. Bailing Jiang, et al. Growth, microstructure and mechanical properties of microarc oxidation coatings on titanium alloy in phosphate-containing solution. Applied Surface Science, 2004, 233:258～267

[56] A.L.Yerokhin, X.Nie, A.Leyland, et al. Plasma electrolysis for surface engineering. Surface and Coatings Technology, 1999, 122:73～93

[57] A.L.Yerokhin, X.Nie, A.Leyland, et al. Characterisation of oxide films produced by plasma electrolytic oxidation of a Ti-6Al-4V alloy. Surface an Coatings Technology, 2000, 130: 195～206

[58] Florian Patcas, Waldemar Krysmann, et al. Preparation of structured egg-shell catalysts for selective oxidations by the ANOF technique. Catalysis Today, 2001, 69:379～383

[59] A.Günterschulze, H.Betz. Neue Untersuchungen über die elektrdytische Ventilwirkung, Z.Phys.，1932 (78): 196～210

[60] A.Günterschulze, H.Betz. Die Elektronenstromung in Isolatoren bei extremen Feldstarken, Z.Phys.，1934 (91): 70～96

[61] K.H.Dittrich, W.Krysmann, P.Kurze, et al. Structure and Properties of ANOF layers, Cryst. Res. & Technol.，1984, 19(1): 93～99

[62] P.Kurze, W.Krysmann, H.G.Schneider. Application Fields of ANOF layers and Composites, Cryst.Res. & Technol.，1986, 21(12): 1603

[63] C. Q. Ning and Y. Zhou, Biomaterials, 2002, 23, 2909.

[64]S. Seuss, A. Chavez, T. Yoshioka, J. Stein and A.R. Boccaccini, Ceram. Trans., 2012, 237, 145. Blend miscibility of poly(3-hydroxybutyrate)and polyethylene oxide) [J]. Polymer, 2004, 45 (2): 453-457

[65]Katajisto J, Linnolahti M, Haukka M, et al. Development of a

Journal of Physical new force field for property prediction of cyclo-olefin copolymers [J]

108(7): 2168-2172 ChemistryB, 2004

[66] Li D X, Liu B L, Liu Y S, et al. Predict the glass transition temperature of glycerol-water binary cryoprotectant by molecular dynamic simulation [J]. Cryobiology, 2008,,56(2): 114-119

[67] J. D. Bumgardner, R. Wiser, P. D. Gerard, P. Bergin,B. Chestnutt, M. Marini, V. Ramsey, S. H. Elder and J.A. Gilbert, J. Biomater. Sci., Polym. Ed., 2003, 14, 423.

[68] C. Aimin, H. Chunlin, B. Juliang, Z. Tinyin and D. Zhichao,Clin. Orthop. Relat. Res., 1999, 366, 239.

[69] Linhui Qianga, Zhanfeng Li a, Tianqi Zhaoa,Atomic-scale interactions of the interface between chitosan and Fe3O4 Colloids and Surfaces A: Physicochem. Eng. Aspects 419 (2013) 125– 132

[70] http://en.wikipedia.org/wiki/Radial_distribution_function